NASA CR-152491

varian

(NASA-CR-152491) PHOTOMULTIPLIER TUBE DEVELOPMENT FOR THE 1.06 MICROMETER WAVELENGTH Final Report, Mar. 1973 - Apr. 1975 (Varian Associates) HC A04/MF A01 CSCL 09A G3/33

N77-22389

Unclas 26017

PHOTOMULTIPLIER TUBE DEVELOPMENT FOR THE 1.06 MICROMETER WAVELENGTH

R.S.Enck Jr.
Varian LSE
601 California Avenue
Palo Alto, California 94303

March 1976

Final Report for Period April 1973 – October 1975

Prepared for

Goddard Space Flight Center
Greenbelt, Maryland 20771

NAS-5-23215

REPRODUCED BY
NATIONAL TECHNICAL
INFORMATION SERVICE
U. S. DEPARTMENT OF COMMERCE
SPRINGFIELD, VA. 22161

TECHNICAL REPORT STANDARD TITLE PAGE

1. Report No. NAS 5-23215	2. Government Acession No.	3. Recipient's Catalog No.
4. Title and Subtitle Photomultiplier Tube Development for the 1.06 Micrometer Wavelength		5. Report Date June 1976
		6. Performing Organization Code
7. Author(s) R. S. Enck, Jr.		8. Performing Organization Report No.
9. Performing Organization Name and Address Varian Associates LSE Division 601 California Ave Palo Alto, CA 94303		10. Work Unit No.
		11. Contract or Grant No.
12. Sponsoring Agency Name and Address NASA Goddard Space Flight Center Greenbelt, Maryland 20771		13. Type of Report and Period Covered Final - March 1973 to April 1975
		14. Sponsoring Agency Code
15. Supplementary Notes		

16. Abstract

This final report covers the development effort directed at the design, fabrication, and testing of high-speed, all-electrostatic photomultipliers for use in 400 megabit laser communication systems operating at the 1.06 μ wavelength. As a direct result of this effort, a high-performance, all-electrostatic III-V photocathode PMT was shown in communication system tests to perform competitively with solid state and avalanche photodiodes. Signal-induced noise and III-V cathode stability were identified as remaining technical problems while cathode quantum efficiencies of $\geq$ 5% at 1.06 μ and 320 picosecond rise and fall time pulse performance were achieved.

17. Key Words (Selected by Author(s)) Photomultipliers Laser communications Solid state photocathodes		18. Distribution Statement	
19. Security Classif.(of this report) UNCLASSIFIED	20. Security Classif.(of this page) UNCLASSIFIED	21. No. of Pages 73	22. Price*

*For sale by the Clearinghouse for Federal Scientific and Technical Information, Springfield, Virginia 22151.

PREFACE

OBJECTIVE

The objective of this program was the development of high-speed, all-electrostatic photomultipliers for use in 400 megabit laser communication systems operating at the 1.06 μ wavelength. The most difficult requirements for this effort were a quantum efficiency requirement for this vacuum PMT of 5% at 1.06 μ and an operating lifetime of 2,500 hours.

SCOPE OF WORK

The work on this program proceeded in two major segments. In the first segment, the conventional cathode all-electrostatic, high-speed PMT developed by Varian LSE on Contract No. NAS5-23110 was further modified to include provisions for the incorporation of 1/4 in. diameter III-V photocathodes. At the same time, a mirror structure InGaAsP photocathode was developed. Following this, tube and cathode technology were combined to produce two deliverable items.

In the second segment, further devices with somewhat higher gain were manufactured for actual communication system testing and also life testing.

CONCLUSIONS

As a direct result of this program, a high-performance, all-electrostatic, III-V high-speed PMT was shown in system tests to perform competitively with solid state diodes and avalanche photodiodes, even though a feedback noise mechanism was present. Major problem areas of the above-mentioned noise and quantum efficiency stability (operating life) were identified. The feasibility of vacuum PMT high-speed receivers operating at 1.06 μ was therefore demonstrated, and the large cathode area of these devices in comparison to solid state detectors make these PMT's attractive for use in high-data-rate laser communication systems.

RECOMMENDATIONS

Further work on both tube and cathode technology are recommended to improve both noise and stability performance. An ion feedback baffled design has received preliminary investigation and indications are that such baffles should eliminate the present feedback noise problem. Stability can be improved through use of better suited dynode materials and also the incorporation of improved (more stable) cathode low work function coatings. Furthermore, Varian has recently developed a hybrid, all-electrostatic PMT which uses an impact ionization diode (IID) in the anode assembly. This tube employs an in-vacuum gain of only 100 and an operating current of less than 1 μA. An additional gain of 100 to 1000 is achieved in the IID. Such a device is a giant step forward in high-speed PMT's; and not only offers much improved stability due to low in-vacuum operating current, but also provides for gain control, without impairing other tube performance, by variation of electron impact potential on the IID.

TABLE OF CONTENTS

Section		Page No.
I.	INTRODUCTION	1
II.	NARRATIVE	2
	A. Phase I – 1.06 μ Sensitive PMT Development	2
	1. Laboratory Research	2
	a. The Mirror Structure Photocathode	2
	b. Research on Cathode Stability	8
	c. Surface Cleaning Experiments	16
	2. Device Development	16
	a. Design Elements	16
	b. Processing	18
	3. Individual Device Performance	28
	B. Phase II – Tube Production for System and Life Tests	42
	1. Device Development	44
	2. Individual Device Performance	48

APPENDIX A: Publications

APPENDIX B: Varian Electron Optics Computer Program

LIST OF ILLUSTRATIONS

Figure No.		Page No.
1.	InGaAsP Photocathode Structure	4
2.	Predicted Quantum Efficiency for a Flatband InGaAsP Photocathode	5
3.	Equilibrium Cs Vapor Pressure vs Time	9
4.	Cs Vapor Pressure During InGaAsP Activation	10
5.	Comparison of Room Temperature and Cooled Yield Curves Showing the Effects of Cooling on an InAsP Photocathode	13
6.	Comparison of the Temperature Dependence of the Heterojunction Barrier Heights for Cs_2O on InAsP and on InGaAsP Samples	14
7.	Comparison of Room Temperature and Cooled Yield Curves Showing the Effects of Cooling to -90° C on an InGaAsP Photocathode	15
8.	Previous Design AEFP	17
9.	Potted AEFP	19
10.	S-20 Cathode Holder Assembly for AEFP	20
11.	III-V Cathode Holder Assembly for AEFP	21
12.	III-V AEFP Electron Optics Plot	22
13.	III-V AEFP Mechanical Design	23
14.	Assembled III-V AEFP Ready for Processing	24
15.	III-V Vacuum Processing System	25
16.	III-V AEFP Pinchoff Assembly	27
17.	Potted III-V AEFP Assembly	29
18.	S/N 003 Pulse Response	30
19.	S/N 003 Cathode Scan at 1.06 μ and (0.63 μ) Laser Wavelengths	31
20.	S/N 003 Gain Scan	32

LIST OF ILLUSTRATIONS (Cont.)

Figure No.		Page No.
21.	S/N 008 1.06 μ Cathode Scan	34
22.	S/N 008 Pulse Response	36
23.	S/N 010 Pulse Response	37
24.	S/N 010 1.06 μ Cathode Scan	38
25.	S/N 012 1.06 μ Cathode Scan	40
26.	S/N 012 Pulse Response	41
27.	Phase I Collector Design	45
28.	Typical Phase I Collector Pulse	46
29.	"Honeycomb" Collector Structure	47
30.	LSE III-V LPE Growth System	49
31.	S/N 027 Output Pulse Response	51
32.	S/N 035 50 μA Output Current Life Test	57

I. INTRODUCTION

This report describes the development of high-speed photomultipliers (PMT's) sensitive to 1.06 μ illumination. The period of performance covered the time span from March 1973 through October 1975. The program, as described in the body of this report, is divided into two phases. Phase I covers the necessary development efforts required to convert an all-electrostatic, high-speed PMT sensitive to visible light (developed under NASA Contract NAS 5-23110) to a 1.06 μ sensitive device. This phase required laboratory research and device development tasks to provide for the appropriate III-V photocathode material development and the necessary tube modifications to incorporate this material. Phase II describes efforts aimed at production of the Phase I designed devices for actual communication system testing as well as life testing.

II. NARRATIVE

A. PHASE I — 1.06 μ SENSITIVE PMT DEVELOPMENT

Over a period of fifteen months, an S-20 five-stage, all-electrostatic, high-speed PMT was developed into a 1.06 μ sensitive device. This was accomplished by a simultaneous two-task effort that independently developed photocathode structures "Laboratory Research" and the tube "Device Development," and then combined the developed technologies to produce working PMTs. The basic S-20 cathode tube design was developed and reported[1] under NASA contract. The following efforts of Phase I were the next step in the long-term development of a 1.06 μ sensitive optical receiver for a 400 megabit-per-second laser communication system.

1. Laboratory Research

The purpose of this task was the development of a 1.06 μ sensitive III-V photocathode destined for use in the PMT structure. The prime cathode material selected for this approach was indium gallium arsenide phosphide (InGaAsP). This cathode system is well described in the literature[2] and needs no description here. The physical cathode size was selected at 1/4" diameter for electron optical reasons. The InGaAsP layer was grown by liquid phase epitaxial techniques on indium phosphide (InP) substrates.

a. The Mirror Structure Photocathode. The quantum yield for a thick negative electron affinity (NEA) photocathode is given by $Y = (1 - R)P/(1 + 1/\alpha L)$ where P is the escape probability, R is the reflectivity, L is the minority carrier diffusion length, and α is the optical absorption coefficient. For operation at the 1.06 μ wavelength, one is forced to make a tradeoff between P and α in choosing the bandgap of the InGaAsP semiconductor material. For a low bandgap (say 1.15 eV), α is sufficiently high that the $(1 + 1/\alpha L)$ term does not decrease the

---

[1] Final Report NAS5-23110

[2] See Appendix A — Central Research Publication Listing

quantum yield too much, but the escape probability P is quite low. For a high bandgap (say 1.21 eV), P is fairly high, but α is so small that αL is less than 1. The optimum compromise at a 1.18 eV bandgap has both α and P at lower than desirable values, resulting in a maximum quantum efficiency of about 5% at the state of technology for this device at the start of this program.

The fact that the InGaAsP quaternary grown by liquid-phase epitaxy forms a good heterojunction with low interfacial recombination velocity with InP allows the construction of a multiple light-pass photocathode structure which can increase the amount of light absorbed and, hence, the quantum efficiency, for a given value of α. The structure of this cathode is shown at the top of Figure 1. A lattice-matching 1.19 eV bandgap InGaAsP layer is grown on an InP substrate. The heterojunction step in the conduction band confines the photo-excited electrons to the active layer. A light-reflecting mirror is evaporated on the polished back surface of the InP substrate. The cathode is then cleaned and activated with Cs_2O by the normal procedures. The relative light intensity throughout the cathode is shown at the bottom of Figure 1. Of the light incident (1) on the photocathode, about one-third is reflected (first incidence reflected light) and two-third enters the active layer. After the first pass through the active layer (2), a significant intensity of light remains (3) which is reflected by the mirror (4) and again passes through the active layer (5). After losing some intensity out of the front surface of the photocathode, the process is again repeated (6, 7, 8 and 9). While somewhat more light is reflected than with a conventional thick active layer cathode (compare total reflected light with first incidence reflected light), the fact that the absorption during step (5) occurs close to the emitting surface rather than deep in a thick conventional layer gives a significant increase in quantum efficiency.

Figure 2 shows the calculated quantum efficiency for a flatband cooled cathode of this type as a function of InGaAsP active layer thickness. A 40% increase in 1.06 μ yield is expected with the InGaAsP thickness optimized with the best values of escape probability.

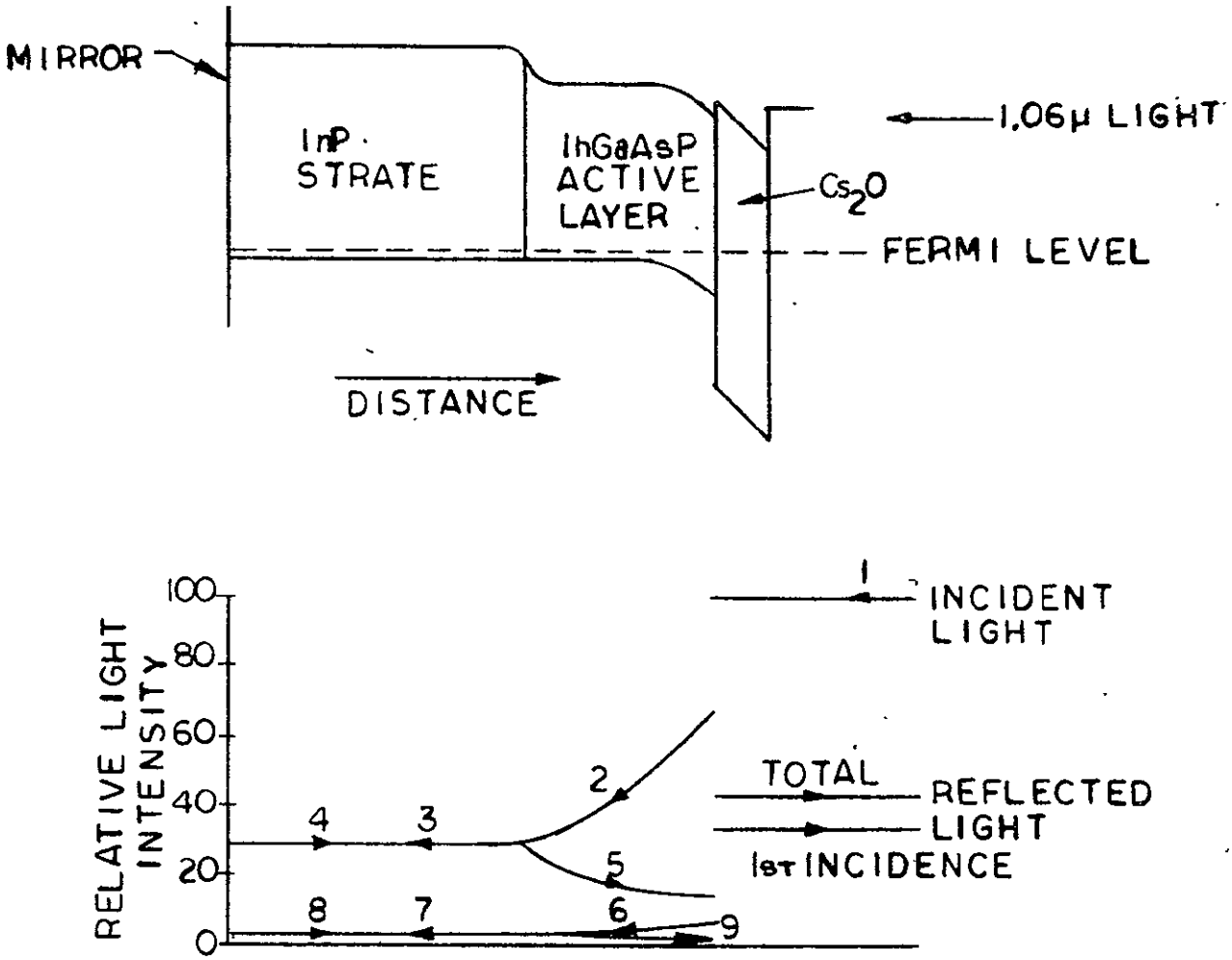

Figure 1. InGaAsP Photocathode Structure. The top figure shows the band diagram for a heterojunction mirror structure photocathode. The horizontal scale represents distance perpendicular to the emitting surface, but is not drawn to scale. The bottom graph has the same distance calibration on the horizontal axis and shows on the vertical axis the relative intensity of the 1.06-micron light on its multiple passes through the photocathode, with the numbered arrows tracing the path.

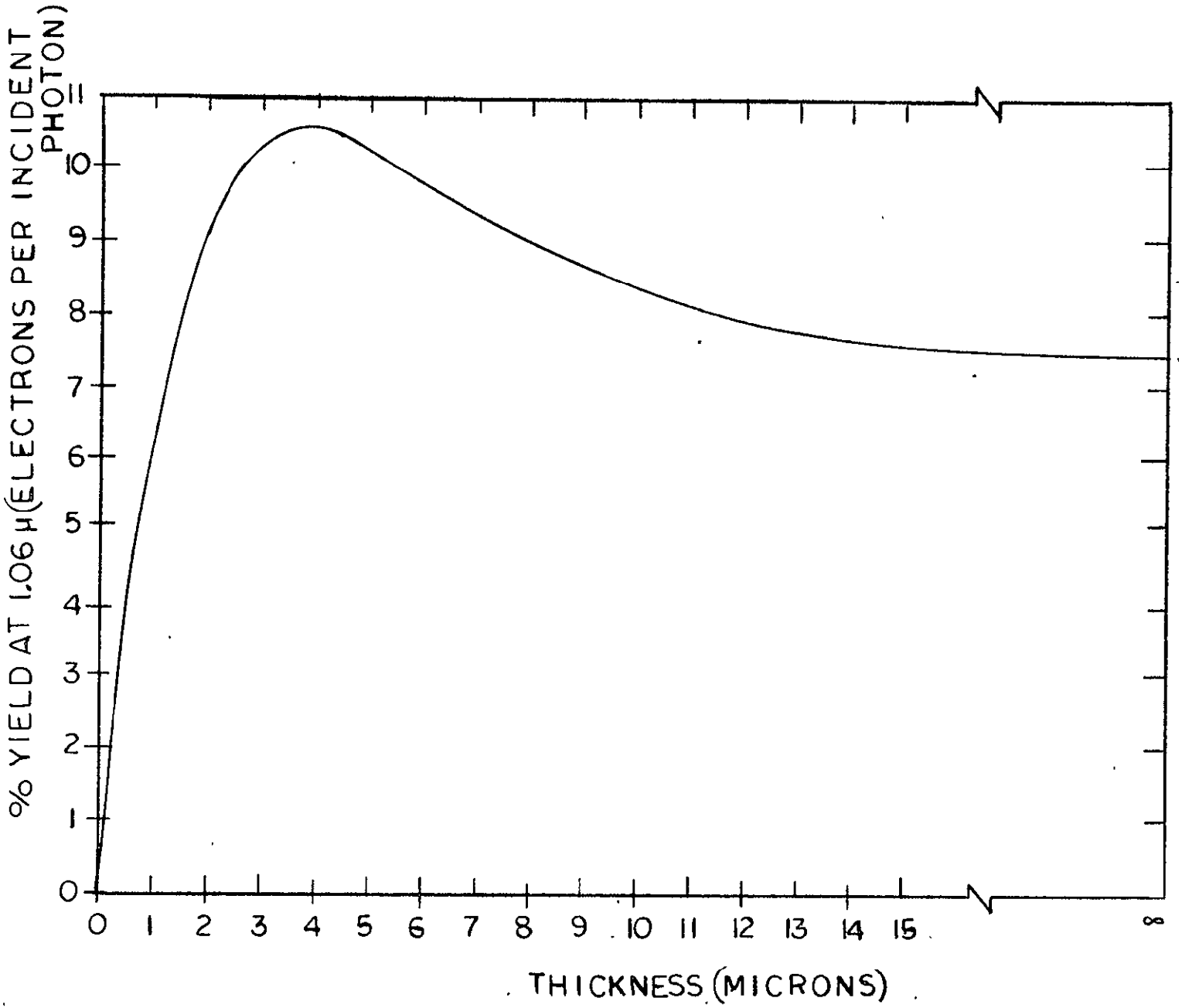

Figure 2. Predicted Quantum Efficiency for a Flatband InGaAsP Photocathode. Predicted quantum yield at 1.06 um vs active layer thickness for the cathode shown in Figure 1. The parameters used for the calculation are h = 1.17 eV, L = 5 um, bandgap = 1.19 eV, interfacial recombination velocity = 0

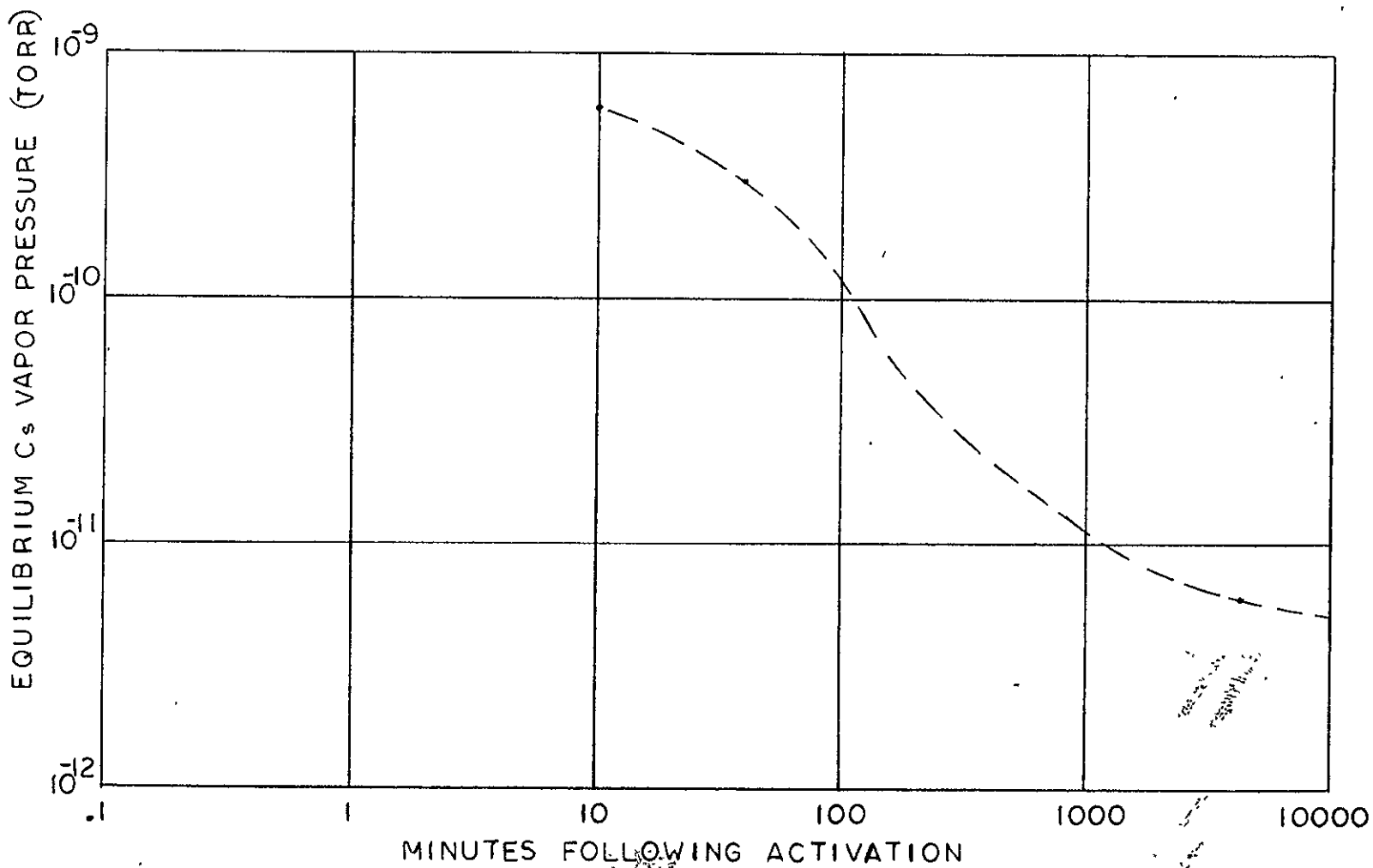

Figure 3. Equilibrium Cs Vapor Pressure vs Time

b. Research on Cathode Stability. Because of the sufficiently high quantum efficiencies obtained from the mirror-structure cathode, the emphasis in the Corporate Research program was shifted slightly. A program to measure the InGaAsP-Cs_2O barrier height as a function of composition with a constant bandgap was temporarily postponed, and a program to measure the time evolution of the Cs partial-pressure gauge was constructed which allowed us to plot independently the Cs and oxygen partial pressures during activation, and to measure the Cs vapor pressure required for stability of an activated cathode. The gauge has a sensitivity of 10 A/torr, allowing us to measure Cs pressures as low as 10^{-14} torr. The first experiment indicated that the equilibrium vapor pressure of Cs over an optimized InGaAsP photocathode is 1-5 x 10^{-13} torr. The results of this investigation will be helpful in stabilizing the cathodes in PMTs at their initial high quantum efficiencies. The Cs pressure required for equilibrium immediately following activation is higher than that required after a few hours. Figure 3 shows a plot of the equilibrium vapor pressure vs time for a 1.06 μ InGaAsP cathode. The quantum efficiency increases somewhat (~ 50%) during this 72-hour process. The equilibrium pressure was measured by keeping the Cs pressure over the cathode adjusted to maintain the cathode at its peak yield point, while measuring that pressure with the Cs partial pressure gauge. This process can be drastically shortened in time by giving the cathode a Cs dump upon the completion of the normal activation. It rapidly comes out of the dump with higher quantum efficiency and the lower Cs over pressure condition. Figure 4 shows the monitoring of an actual activation using the Cs dump process. Apparently a cathode should be kept at its optimized sensitivity in the processing station for the 2 to 3 hours in which the equilibrium Cs vapor pressure is dropping before being transferred into the tube, which would be preactivated to provide the proper final equilibrium vapor pressure.

The resultant Cs vapor pressure following either the dump or the 72-hour wait is still high enough, when combined with the fact that 0.004 micro-torr seconds of Cs overexposure will reduce the sensitivity by 20%, that a cathode in a clean tube should die with a time constant of about 50 minutes. If a lifetime (to 1/e) of 10 years is desired, then the initial Cs vapor pressure in the tube would

Having completed the theoretical optimization of the semiconductor portion of the cathode, effort was concentrated on designing the mirror portion of the mirror-structure cathode. It was initially thought that a dielectric mirror would cause the least interference with established processing procedures and would insure high reflectivity at 1.06 μ after passing through all the processing steps. The reflectivity of a simple, alternate, quarter-wave mirror of SiO_2 and Si_3N_4 on InP is given approximately by $R = (A-4)/(A+4)$ where $A = 7 \times 2^m$ and m is the number of pairs of SiO_2, Si_3N_4 layers. For four pairs a reflectivity of 93% is expected. A four-pair layer requires about 2 hours to deposit in the CVD reactor, but many cathodes can be coated simultaneously. Growth parameters for a 1.06 μ quarter-wave layer of both SiO_2 and Si_3N_4 were determined, and the structure grown. The resulting structure was too thick, and cracked upon cooling to room temperature.

Thus, other material systems were examined which would have high reflectivity and which would neither degrade the photocathode performance nor be degraded itself by the substrate B-face preparation, the epitaxial layer growth, or the heat cleaning. A solution which satisfies all the necessary conditions was finally reached. All InGaAsP active layers for the tubes on this contract were grown on the following substrate formed by coating the A-face of InP to give the desired mirror properties.

(1) Mechanically polished 1/4" diameter InP approximately 200 μ thick

(2) Phosphosilicate glass approximately 300 Å thick

(3) Silicon nitride approximately 600 Å thick

(4) Quartz approximately 250 Å thick

(5) Chrome approximately 2000 Å thick

(6) Quartz approximately 250 Å thick

(7) Silicon nitride approximately 600 Å thick

Following the adjustment of the melt composition in the mirror-structure cathode growth system, consistently good cathodes were grown for tube processing.

This flatband calculation is adequate to estimate the obtainable performance, but not to calculate the optimum parameters for the real situation where the bandgap is graded. Photocathode yield has, in general, been calculated by solving the one-dimensional electron transport differential equation, given the front and back surface boundary condition. Using a Green's function approach, this was extended to the case of a linear gradient in bandgap. Any further generalization results in an equation for which no solution is readily apparent. The real case required a further generalization, so a lumped element model of the photocathode was devised and solved using circuit techniques. The computer program using this method of solution, while taking much more computer time than simpler solutions, can properly handle any arbitrary variation of bandgap and diffusion length as a function of epitaxial layer thickness.

The actual bandgap gradient profile as a function of thickness was measured for the then current InGaAsP growth conditions. The optical transmission of samples of several thicknesses was simultaneously measured. The optical absorption coefficient as a function of bandgap and photon energy was calculated from the measured optical transmission to be self-consistent with the measured grading (which involves integrating α through the layer since α is a function of position). Finally, these measured values of α and bandgap gradient were used to calculate the quantum yield expected from the mirror structure cathode as a function of epitaxial layer thickness for the current growth conditions and for various modified growth conditions. The results of this study showed that a small change in current melt composition would give a 7% improvement in projected mirror structure 1.06 μ quantum yield, while a complete revision of the growth parameters oriented towards reducing or eliminating the bandgap gradient after one or two microns of growth would produce a 22% improvement. These calculations also gave us, of course, the desired epitaxial layer composition and thickness for best mirror structure performance. The bandgap gradient present in the early liquid-phase epitaxial (LPE) photocathode structure is clearly detrimental to performance, with or without the mirror present. A new growth schedule involving a slower cool-down cycle was introduced to reduce the gradient. This required reoptimization of the Zn doping.

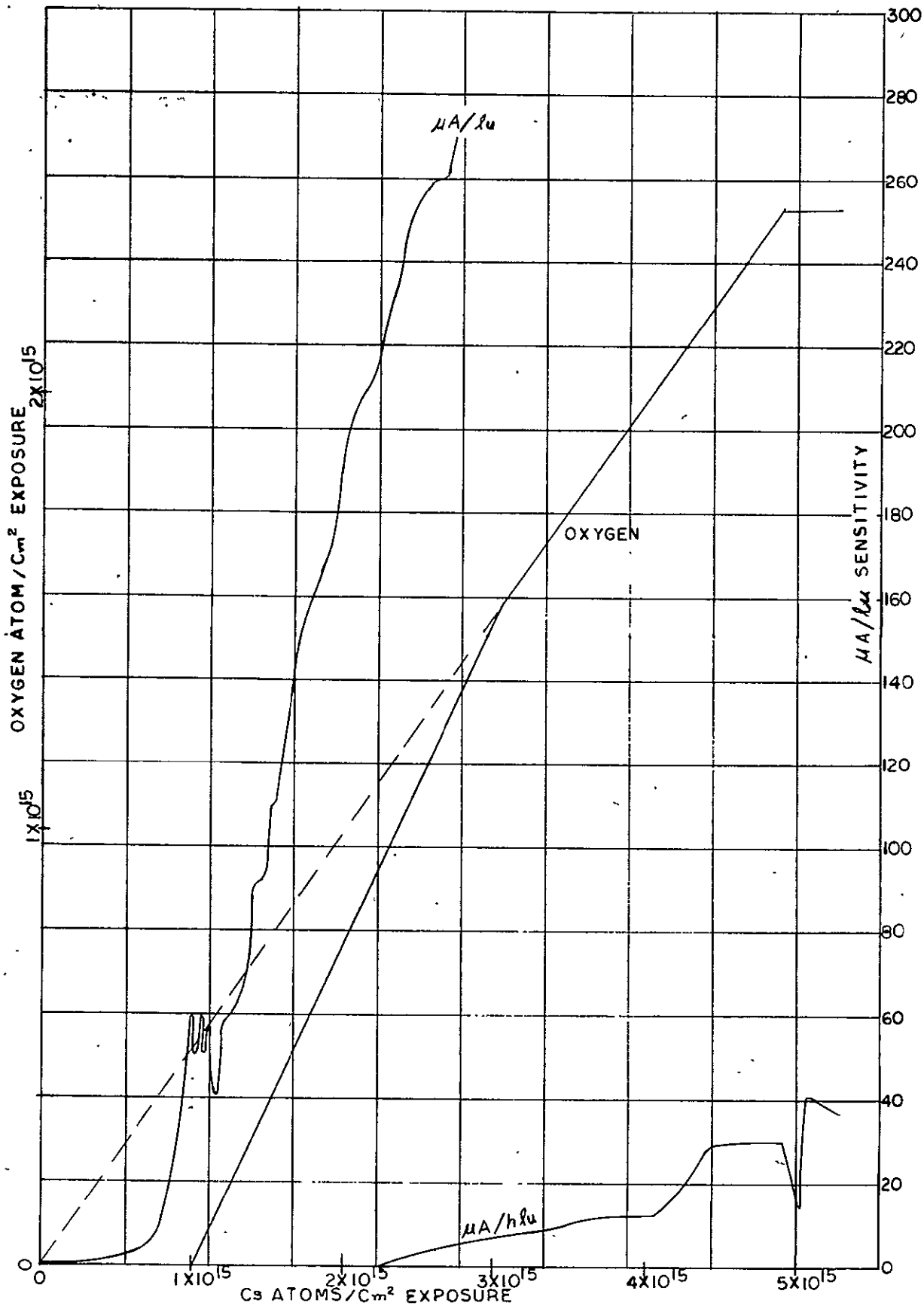

Figure 4. Cs Vapor Pressure During InGaAsP Activation

have to be correct to 1 part in 10^5 (assuming that the long-term behavior is the same as that of the short term). It seems more likely that the cathode sensitivity will level off at some lower value where its Cs vapor pressure corresponds to that of the tube, but the magnitude of the preprocess-stability problem is seen to be enormous. Cooling, which experimentally lowers all of the vapor pressures involved and, hence, extends the lifetime of an off-balance tube, may be the only viable alternative to an active system which, using feedback control circuitry, adjusts the oxygen or Cs vapor pressure in the tube to keep the cathode at its peak sensitivity.

Operation at Other than Room Temperature. Many of the parameters of III-V photocathode operation are affected by the cathode temperature. Since heating or cooling by a moderate amount is easily implemented, temperature should be considered a legitimate variable in optimizing performance. Heating above room temperature by more than about 20°C produces such a rapid loss of Cs from the cathode surface that operation with heating is rejected as undesirable. Cooling has been shown to produce, both theoretically and experimentally, the following effects:

(1) The bandgap of the III-V material increases.

(2) The optical phonon energy for III-Vs is near kT at room temperature. Thus, cooling will reduce optical phonon electron scattering, which will reduce scattering in the band-bending region and will increase the minority carrier diffusion length, L.*

(3) The photocathode dark current is decreased, as the electrons causing the dark current are thermally excited.

Effect (1) is easily compensated for by growing the III-V material to have the proper bandgap at the desired operating temperature. The shift of bandgap with temperature is well known quantitatively for III-V semiconductors.

---

*This is true for L only down to a certain temperature, usually 100-150°K, due to other factors affecting the diffusion length.

Effects (2) and (3) are both desirable effects in improving the photocathode operation.

The effect of cooling on the interface heterojunction parameters is not theoretically understood. Changes in Cs_2O work function with temperature would not appear to be a problem, as S-1 photocathodes are successfully operated in a cooled mode and the Cs_2O thickness is easily optimized for cooled operation of a III-V photocathode. Thus, an increase in the heterojunction barrier height upon cooling is the only possible adverse effect which could cancel out the other gains obtained.

For InAsP, the barrier height has been measured to be independent of temperature. The electron transmission probabilities T_{BS}, T_{ABS}, and T_{BV} are also temperature-independent. Thus, the only advantages obtained from cooling InAsP are slightly longer diffusion length and a reduced dark current. Figure 5 shows the quantum yield curves at room temperature and with cooling for an InAsP sample (bandgap too high for 1.06 μ operation).

Measurements of the barrier height variation with temperature for InGaAsP show that the barrier behavior is more favorable for the quaternary (shown in Figure 6), as cooling produces a reduction of about 70 mV in the barrier. The threshold plots show that T_{ABS} and T_{BV} remain constant, but T_{BS} is increased dramatically. Shown in Figure 7 are the quantum yield curves for room temperature and cooled operation of an InGaAsP sample. The 1.06 μ yield at room temperature was 4.2%, with the bandgap being too low for optimum 1.06 μ yield. Upon cooling, the 1.06 μ quantum efficiency increased to 7.5%. This was the highest 1.06 μ quantum efficiency yet measured. The bandgap was probably a little high for optimum cooled operation, so further improvements can be expected with further work.

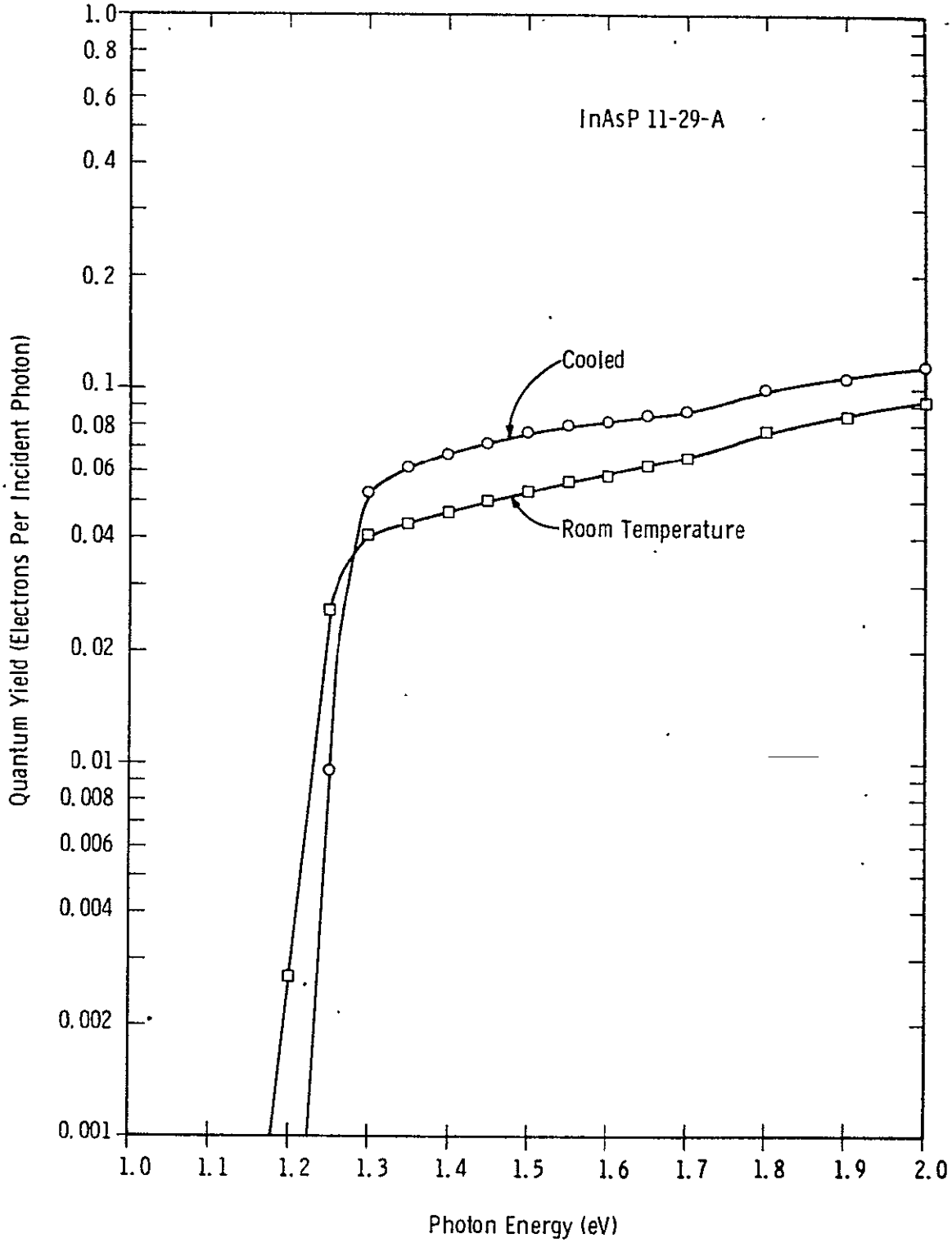

Figure 5. Comparison of Room Temperature and Cooled Yield Curves Showing the Effects of Cooling on an InAsP Photocathode

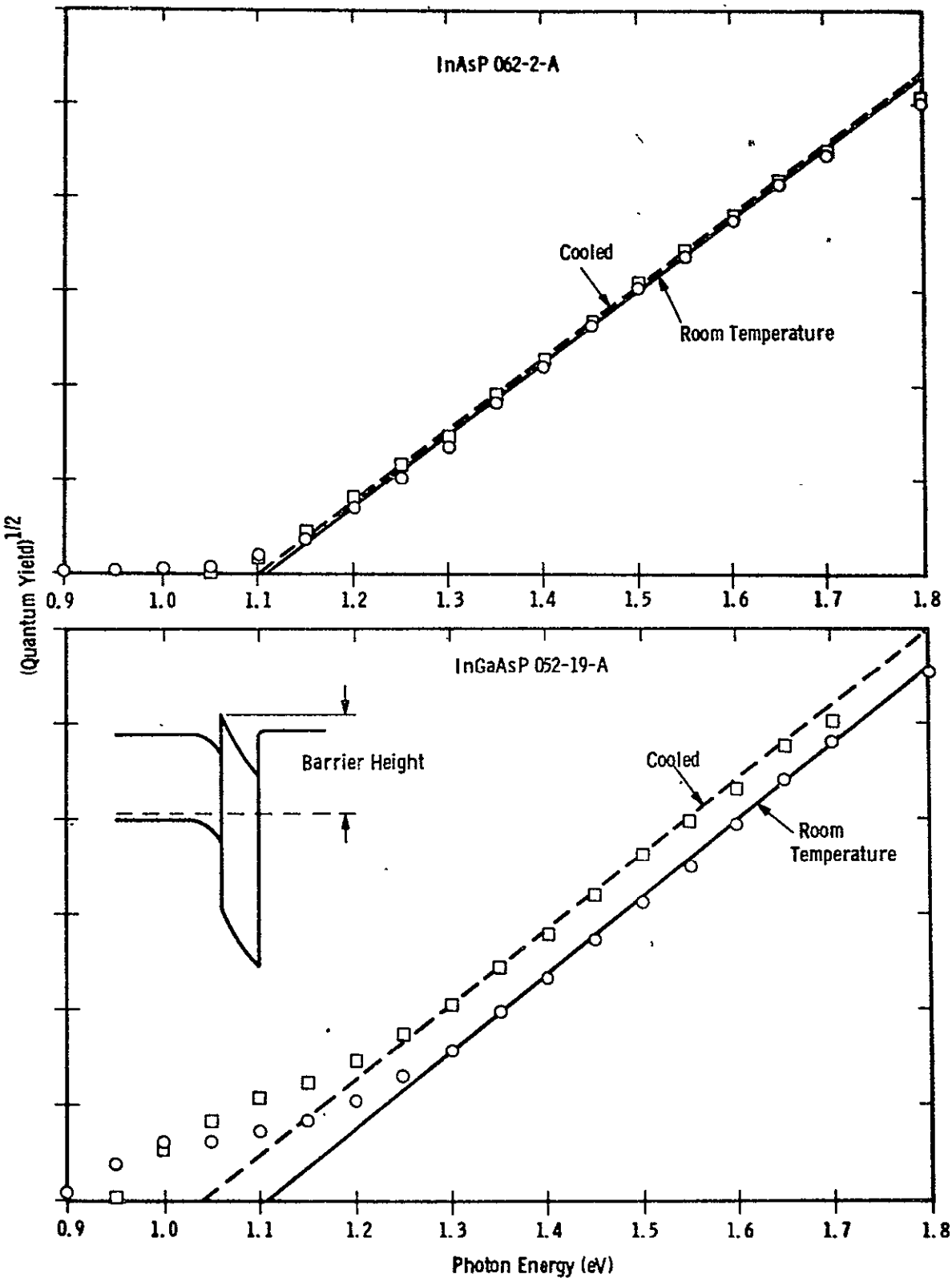

Figure 6. Comparison of the Temperature Dependence of the Heterojunction Barrier Heights for Cs_2O on InAsP and on InGaAsP Samples. As shown in the lower insert, low bandgap p-type samples (~0.8 eV bandgap) were used for both measurements. The barrier height is given by the extrapolated x-axis intercept of the straight line segment of the (Yield)$^{1/2}$ plot.

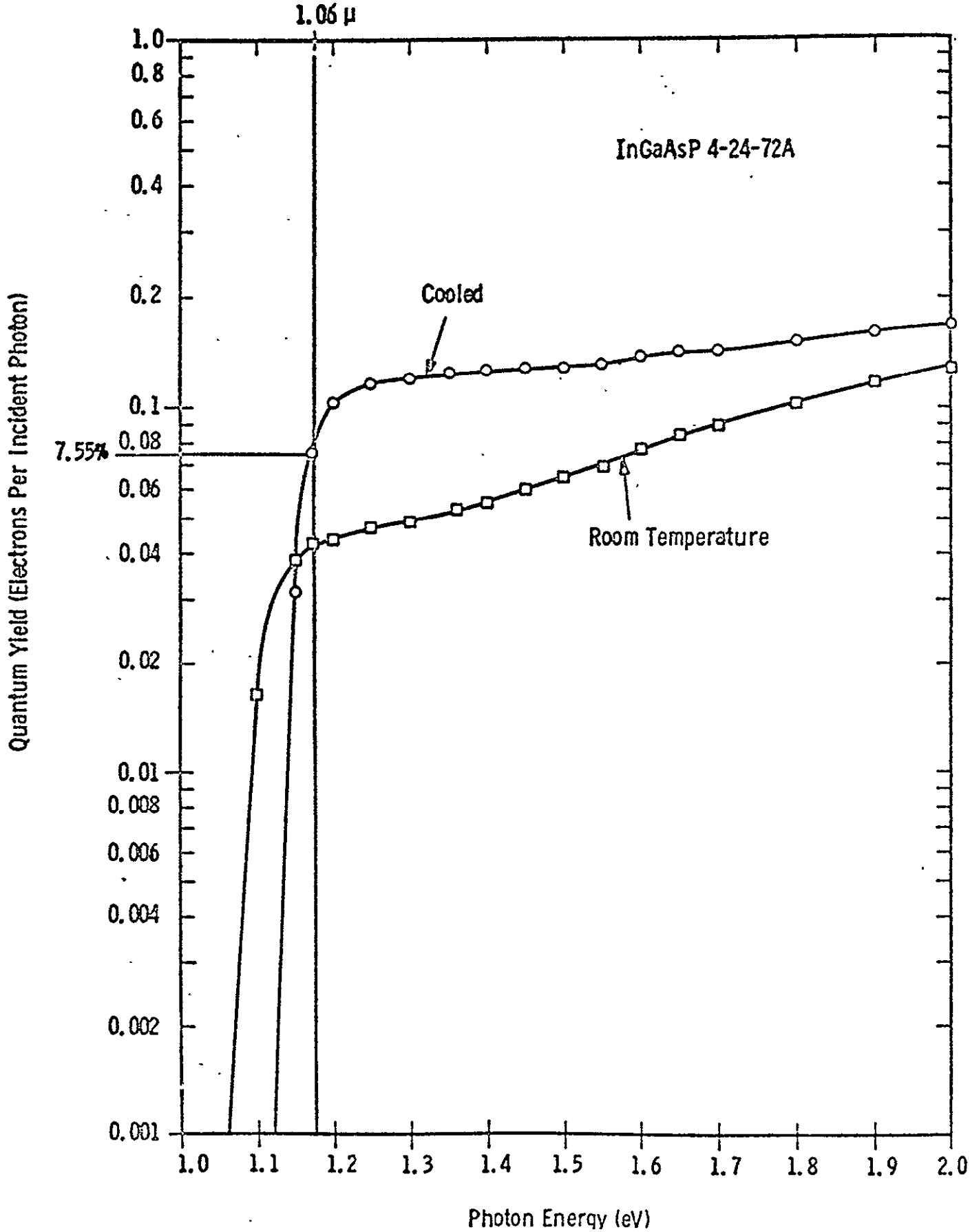

Figure 7. Comparison of Room Temperature and Cooled Yield Curves Showing the Effects of Cooling to -90° C on an InGaAsP Photocathode.

c. Surface Cleaning Experiments. The normal heat cleaning procedure leaves the surface in a certain configuration which is determined by surface interactions at the highest heat cleaning temperature. This may not be the surface configuration which would give the lowest heterojunction barrier or the highest quantum yield. Heat cleaning does an adequate job of cleaning the surface, but the surface can also be cleaned by using ion bombardment to sputter away several monolayers of material. This leaves a clean but disordered surface due to ion bombardment damage. In order to make this a useful technique, a method must be found to anneal out the damage without reverting to the equivalent of a heat cleaning process. Several experiments were tried using two different samples. Very low ion energies and nearly grazing incidence were used to keep the damaged region as shallow as possible. Following the ion bombardment treatment, the layer consists of single crystal with a very thin top layer of amorphous material. In the case of ion implantation damage in other semiconductors, it is known that the amorphous material can regrow epitaxially on the single crystal base at low annealing temperatures. However, this did not occur in our experiments. Even at temperatures 100°C below the normal heat cleaning temperature, phosphorous is lost from the amorphous layer, leaving a layer more closely resembling the melt from which the original material was grown than the original single crystal. There is no way to recover proper stoichiometry once the P loss occurs. Needless to say, the photoemission performance of the resulting surface is very poor. It is quite similar to the performance from polycrystalline material deposited by vapor epitaxy on a foreign substrate.

2. Device Development

a. Design Elements. This tube development effort was aimed at incorporating a spring locking crystal holder into the previously designed all-electrostatic fast PMT (NASA Contract No. NAS 5-23110). Figure 8 depicts this previous design. This structure is a "cup and slat," all-electrostatic device, which was computer designed to enable an anode pulse rise time of less than 1 nanosecond. The five-dynode structure produces about 5×10^3 gain and had a

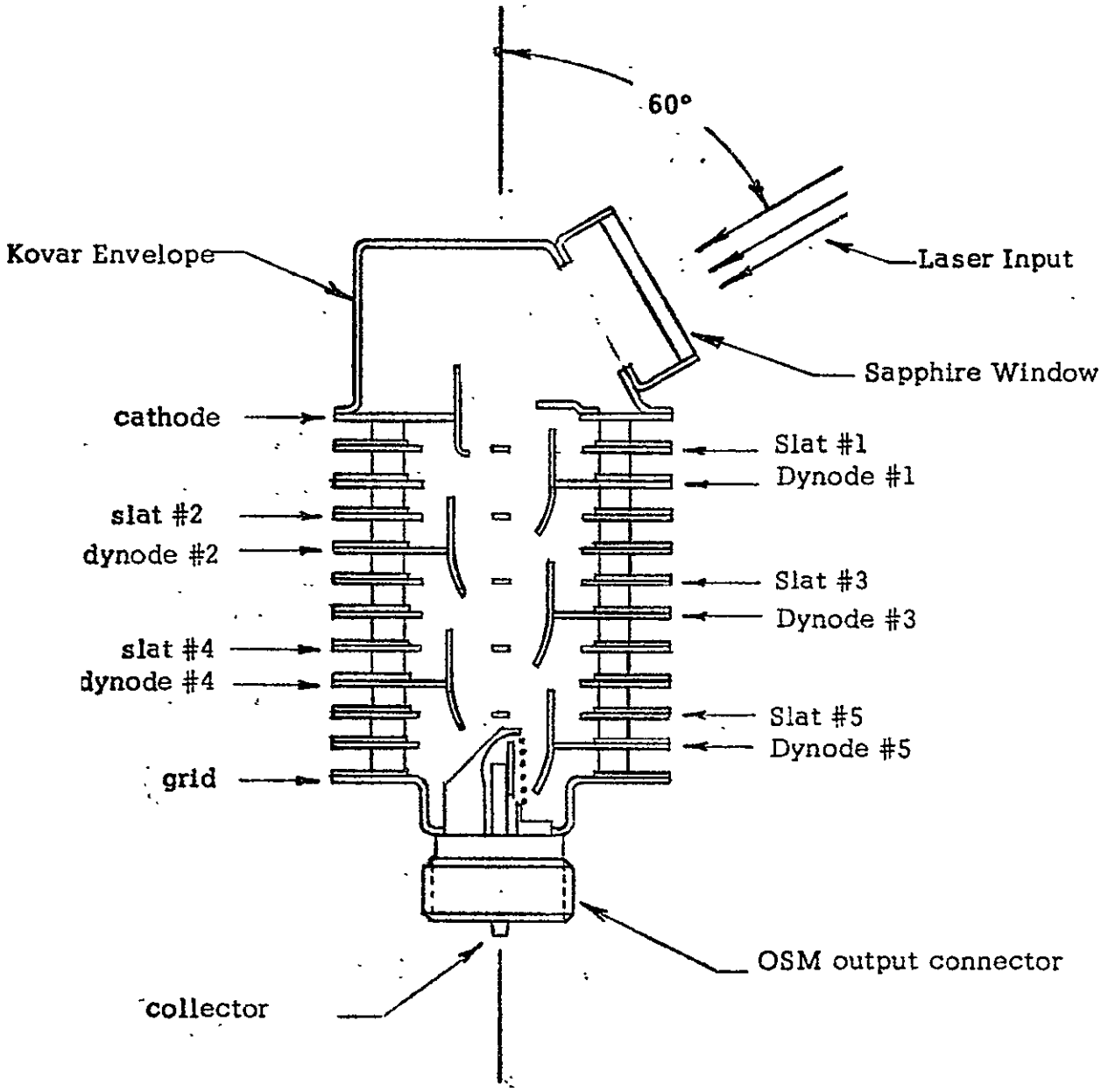

Figure 8. Previous Design AEFP

planer cathode structure to simulate the upcoming incorporation of planar III-V photocathodes. The encapsulated dimensions for this tube are shown in Figure 9, which shows the potted tube assembly. Figure 10 shows the actual cathode structure layout which required redesign to ruggedly mount a 1/4" diameter III-V cathode (as described above) without perturbing the electron optics design of the remaining tube structure. The III-V cathode holder design appears in Figure 11. The electron optics of this structure as mounted in the tube "front" end were verified on Varian's digital computer electron optics program (see Appendix B) and a Calcomp electron optics plot is shown in Figure 12. Here, cathode electrons are injected with 1 eV of energy at angles normal and both + and - 45° to the surface to simulate worst case cathode electron injection conditions (actually, for InGaAsP, the electron injection energy spectrum is only a small portion of an electron volt and emits within 5 to 10% of the normal). This electron optics evaluation confirmed that the whole cathode surface would be useful and produce an output pulse easily fast enough for 400 mb/s optical communication.

A complete III-V, all-electrostatic, high-speed PMT was drawn from this investigation. A cross section of the mechanical design is shown in Figure 13. The completed structure is constructed using basically ceramic-to-metal brazed seals on heliarc welded flanges, which have been proven in the vacuum devices to yield the ultimate in a reliable, rugged tube.

b. Processing. The assembled tube, ready for vacuum processing, is depicted in Figure 14. Here the basic tube has appended a silver leak tube (acting as an oxygen source), a Cs generator, and a transfer tabulation terminated with a Varian Conflat® flange. This exhaust assembly is affixed to a III-V vacuum processing system as shown in Figure 15. This vacuum station serves as the mechanism enabling tube vacuum processing as well as III-V photocathode processing and subsequent transfer into the tube. After the tube is bolted onto the vacuum system "main chamber," the system is evacuated and both tube and system are baked overnight.

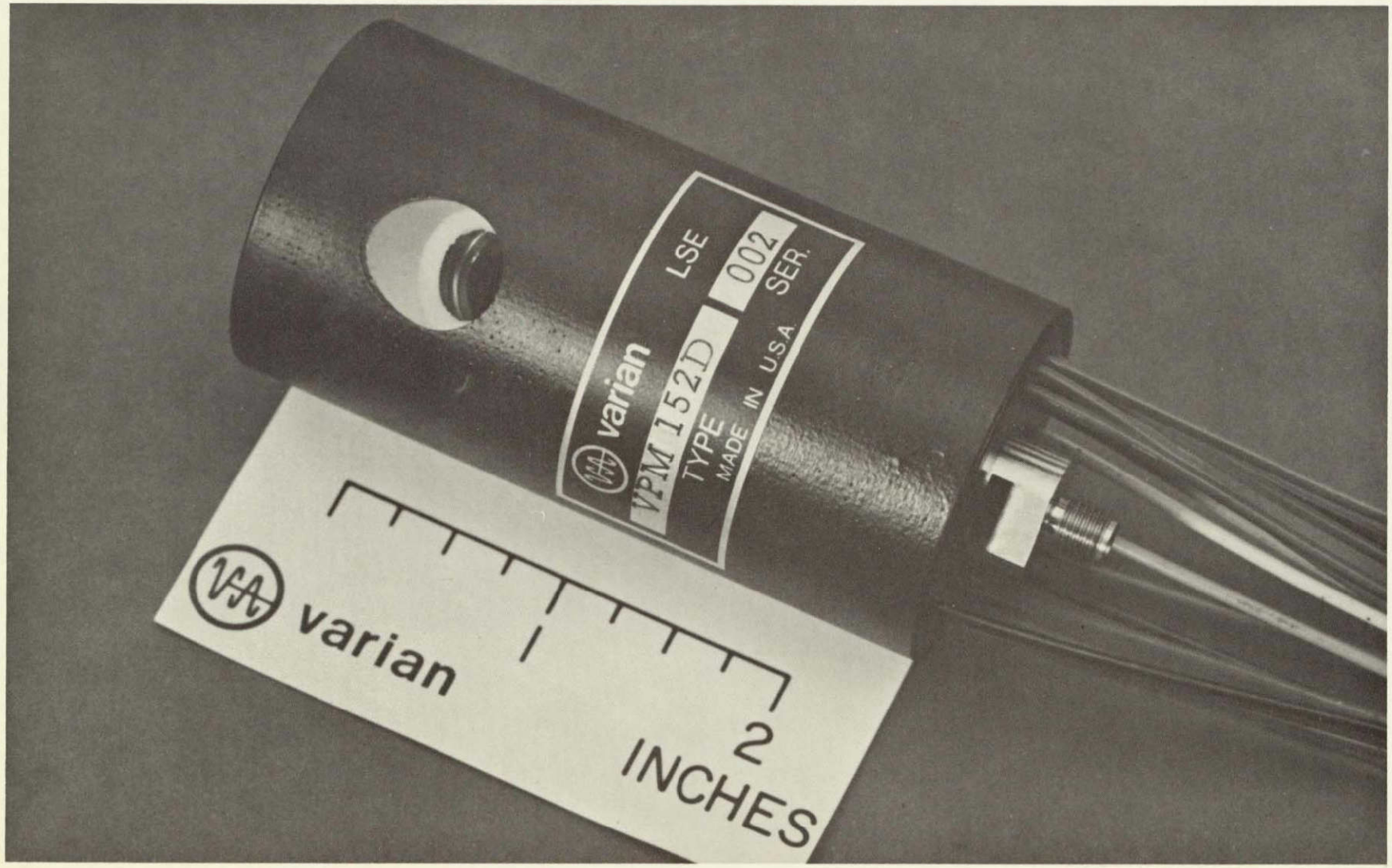

Figure 9. Potted AEFP

REPRODUCIBILITY OF THE
ORIGINAL PAGE IS POOR

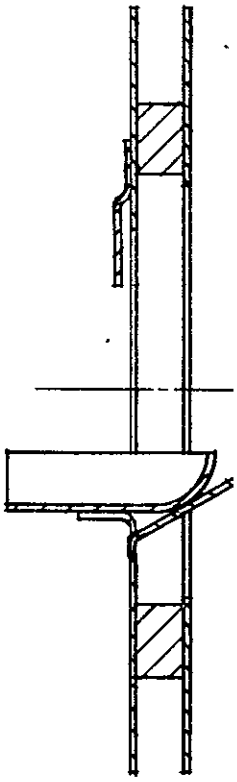

Figure 10. S-20 Cathode Holder Assembly for AEFP

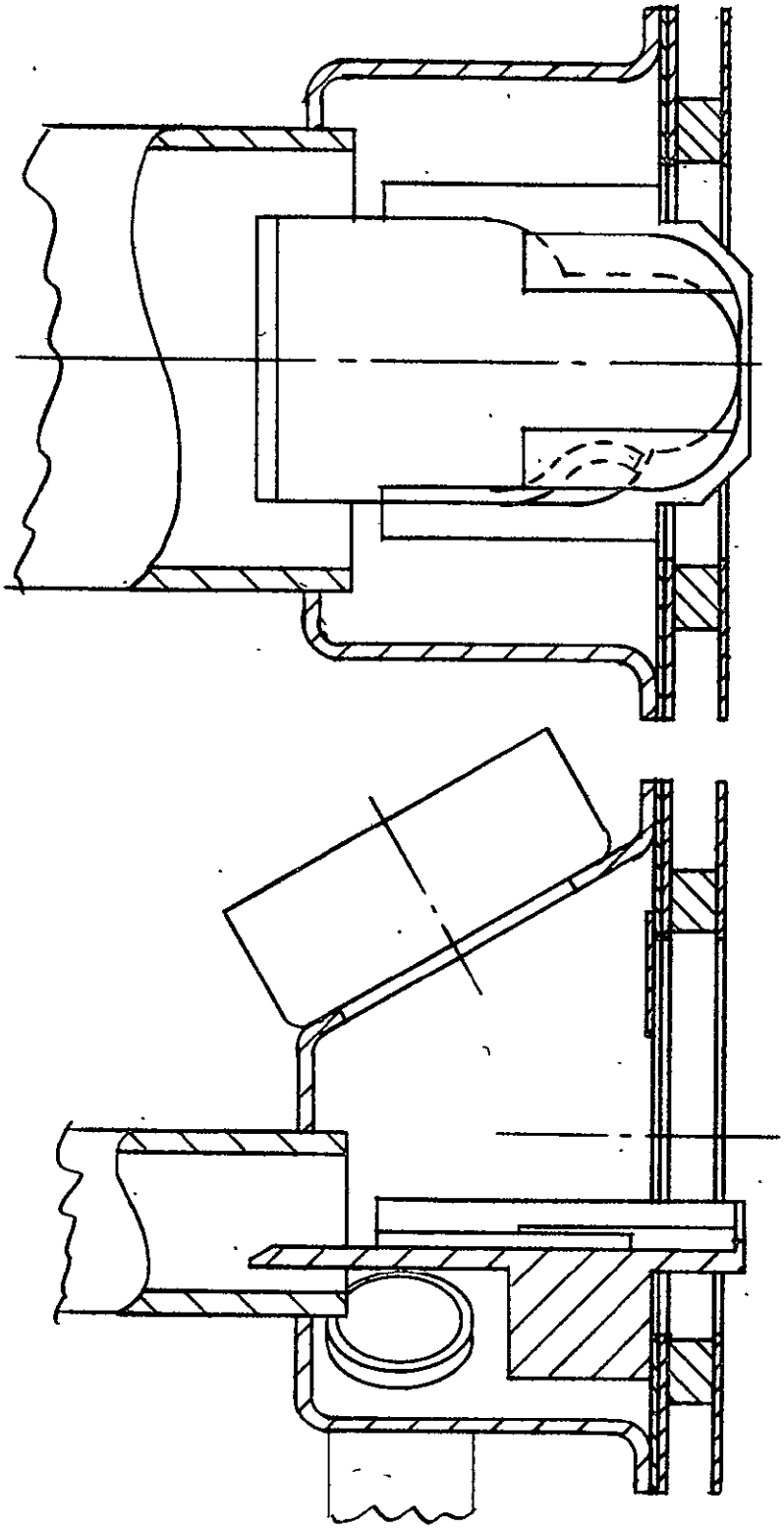

Figure 11. III-V Cathode Holder Assembly for AEFP

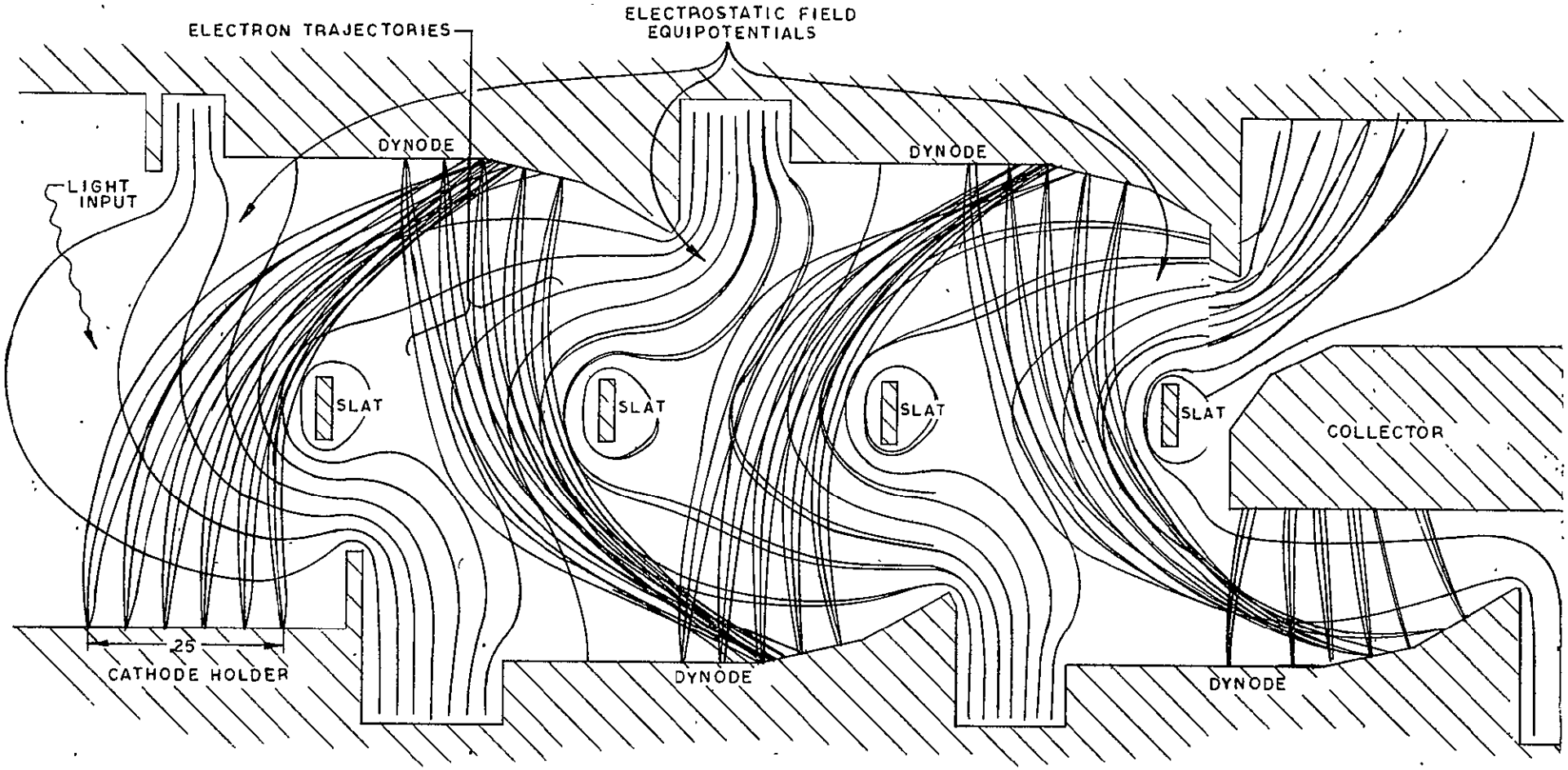

Figure 12. III-V AEFP Electron Optics Plot

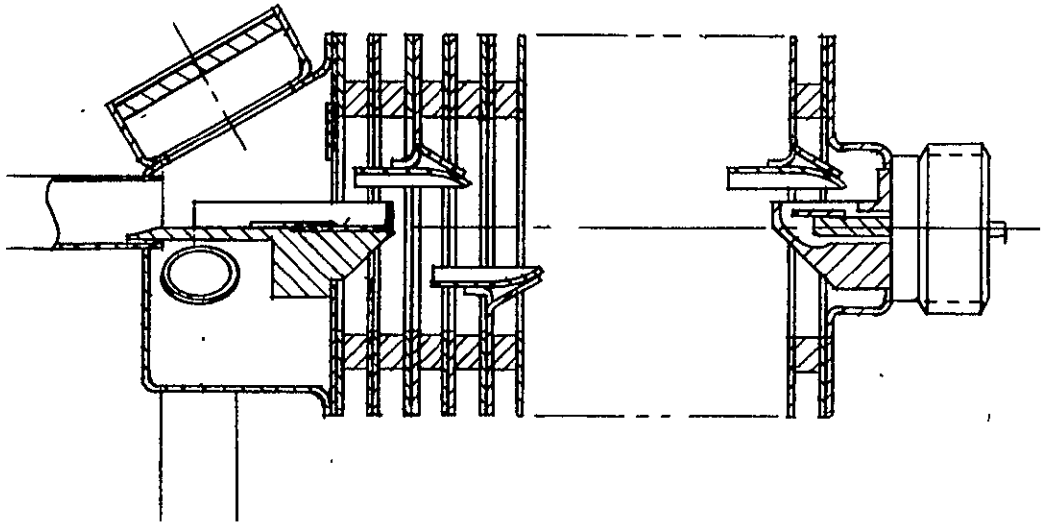

Figure 13. III-V AEFP Mechanical Design

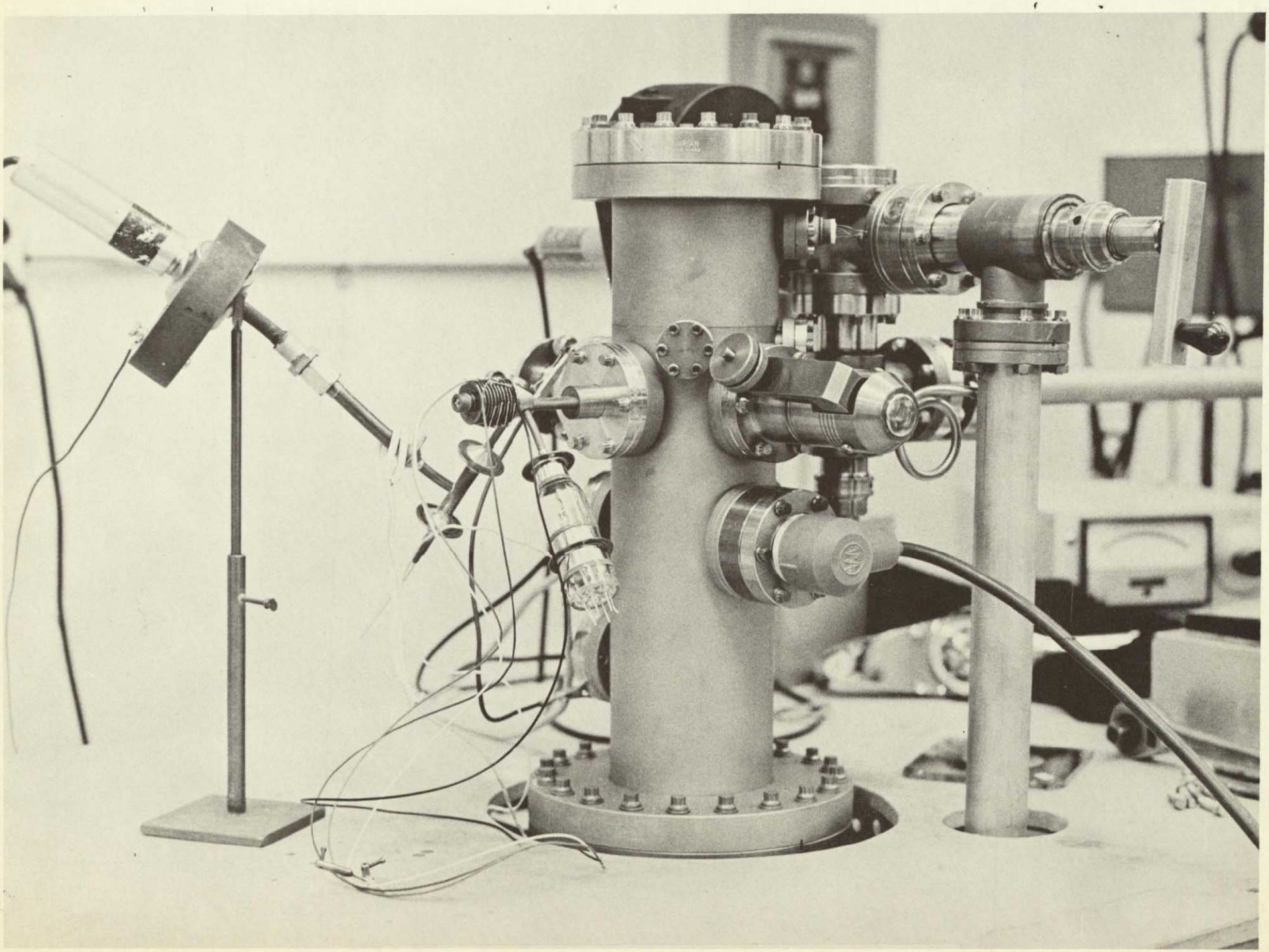

Figure 14. Assembled III-V AEFP Ready for Processing
(Mounted on vacuum station)

REPRODUCIBILITY OF THE
ORIGINAL PAGE IS POOR

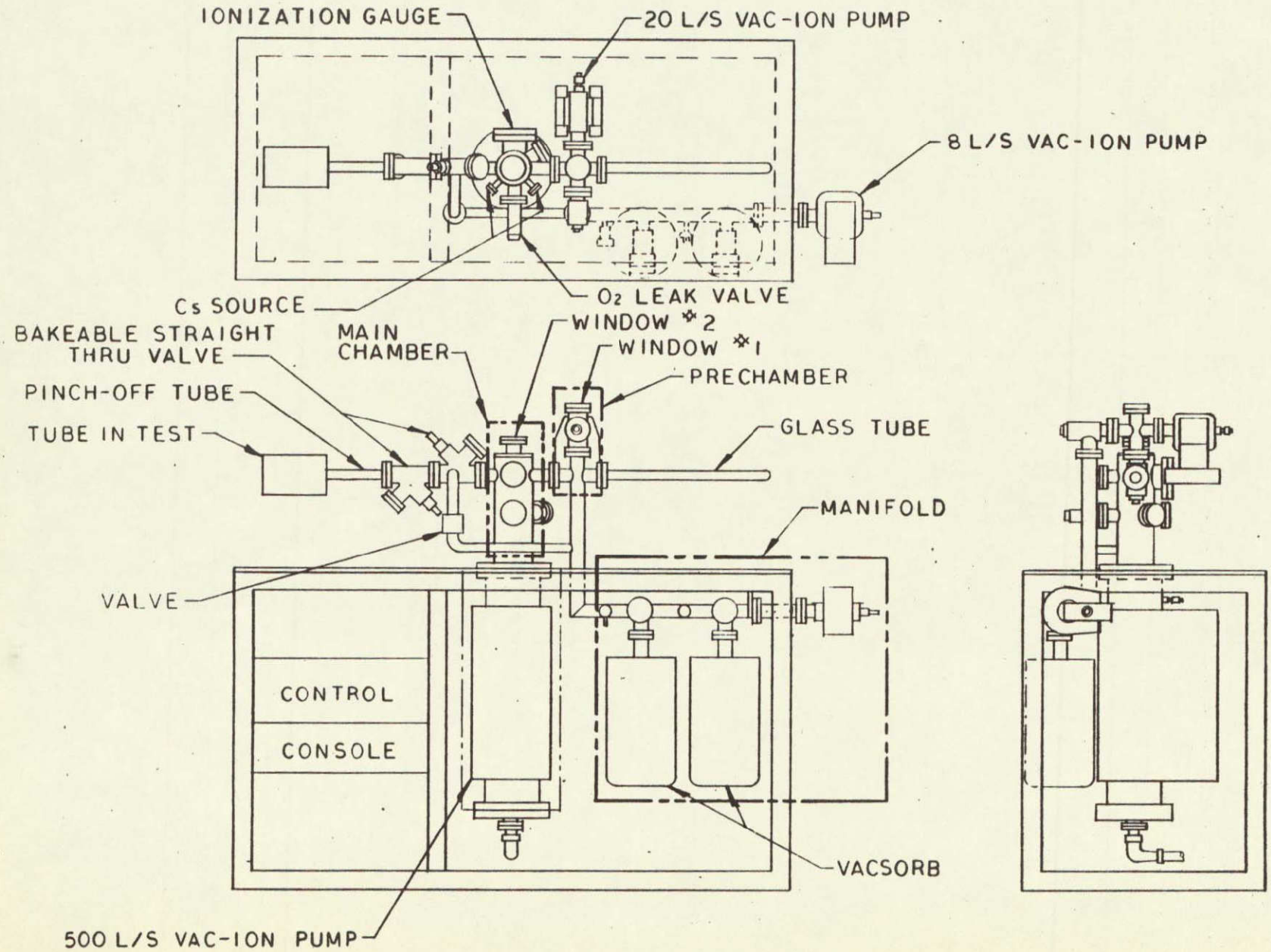

Figure 15. III-V Vacuum Processing System

On the next morning, the tube and system are cooled achieving 10^{-11} torr vacuum in the main chamber. The tube is then preprocessed to establish the proper partial pressure of Cs within the device for good cathode stability. Then, using ultraviolet (UV) illumination to excite photocathode current, the tube is tested for gain and dark current. The test is followed by an operational scrub to reduce outgassing during the tube's operating life. This process is essential, since such outgassing will rapidly kill III-V photocathodes.

Upon completion of scrubbing, gain and dark current are remeasured and, if these values are acceptable, the tube is designated as ready for cathode insertion. At this point, a chemically cleaned and polished 1/4" diameter cathode (InGaAsP) is placed into the prechamber (see Figure 15). The prechamber is pumped to high vacuum until its valve can be opened to the main chamber. An 8ℓ per second Vacion® pump is used for this purpose, while rough pumping is done through the manifold system using Vacsorb® (cryogenic) pumps. After opening the prechamber to the main chamber, the cathode is transferred, using a magnetic fork assembly, to the main chamber where it is heat cleaned just to the point of decomposition and then activated with Cs_2O. If acceptable quantum efficiency is achieved by this process, the cathode is then transferred into the awaiting tube assembly. If poor cathode yield results, the cathode is brought back to the prechamber and removed to allow for placement of a new cathode. After transferring a good cathode into the tube, the tube is pinched off the vacuum system using a copper cold-weld technique. This pinch-off assembly is shown in Figure 16. Note at this point that the Cs and oxygen generators are still in place to allow for cathode "tweeking" should degradation occur.

The tube assembly is monitored next by routine measurements of its general infrared sensitivity (7000 Å and up) by reading cathode current in response to illumination through a Corning No. 2540 filter. The result is a reading of tube sensitivity expressed in microamps per hollow lumen ($\mu A/_{hlu}$). This measurement technique has been accepted rather than using quantum efficiency at 1.06 μ

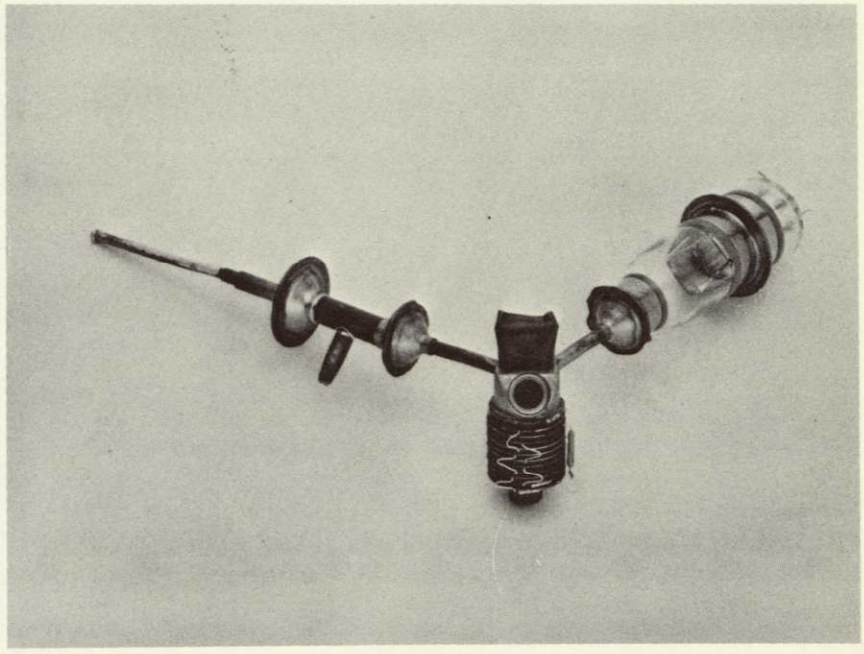

Figure 16. III-V AEFP Pinchoff Assembly

REPRODUCIBILITY OF THE
ORIGINAL PAGE IS POOR

because it utilizes higher cathode current levels and is, therefore, an easier and more accurate monitoring measurement. If the sensitivity is stable over a period of a few days, then an operational scrub at 50 μA of collector current is performed to ascertain the operating stability of the tube. After this, the assembly is ready for Cs and oxygen generator pinch off, followed by vacuum potting, final test and delivery. The final tube assembly is pictured in Figure 17.

3. Individual Device Performance. A total of eleven tube starts were made under this phase. A start is defined as the placement of a tube assembly on the exhaust system for bakeout. Each start is individually addressed below.

S/N 003. This tube was started on 7/26/73 and removed from station on 8/9/73 with a 3% at 1.06 μ cathode. DC gain performance was excellent, with 7×10^3 gain and about 60% collector efficiency. Cathode stability was very poor for this tube due to an excessive partial pressure of Cs within the tube (nonoptimal preprocess). Over one weekend, response degraded to only 0.04% at 1.06 μ and about 9% QE at 0.53 μ from an original 14%.

In late September, McDonnell-Douglas tested the tube. Pulse response is shown in Figure 18. The long pulse tail resulted from the presence of high secondary emission surfaces within the collector structure. Gold plating of this area was therefore planned. Figures 19 and 20 show cathode and gain scans, respectively. The mountainous 1.06 μ cathode scan was probably the result of severe cathode degradation. However, the duplication of this mountainous format in the gain scan indicated excellent gain uniformity across the entire 1/4" diameter cathode surface.

S/N 005. This tube was started on 8/23/73, but was scrapped due to a copper tubulation fracture which occurred after bakeout.

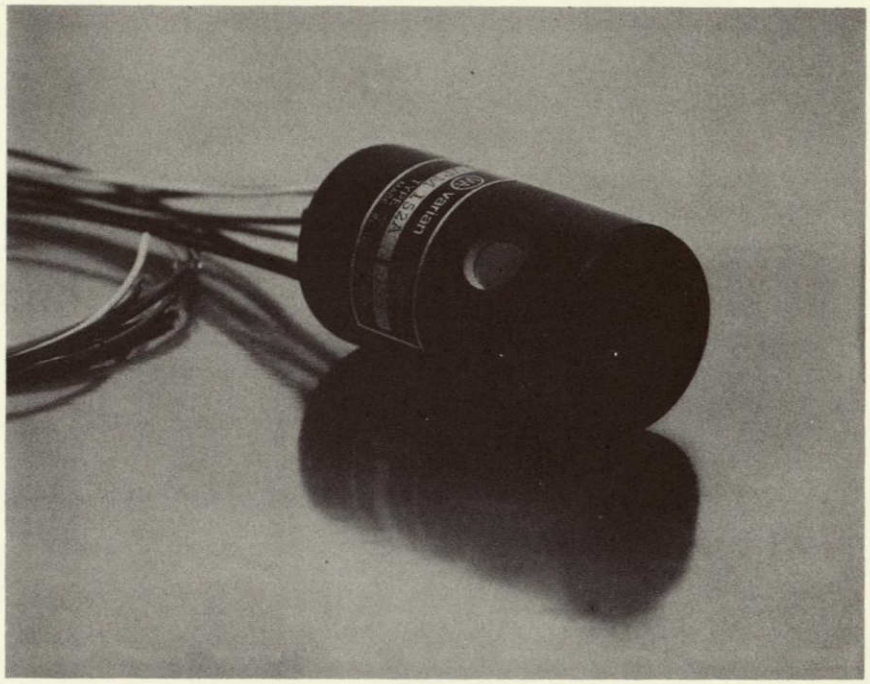

Figure 17. Potted III-V AEFP Assembly

REPRODUCIBILITY OF THE
ORIGINAL PAGE IS POOR

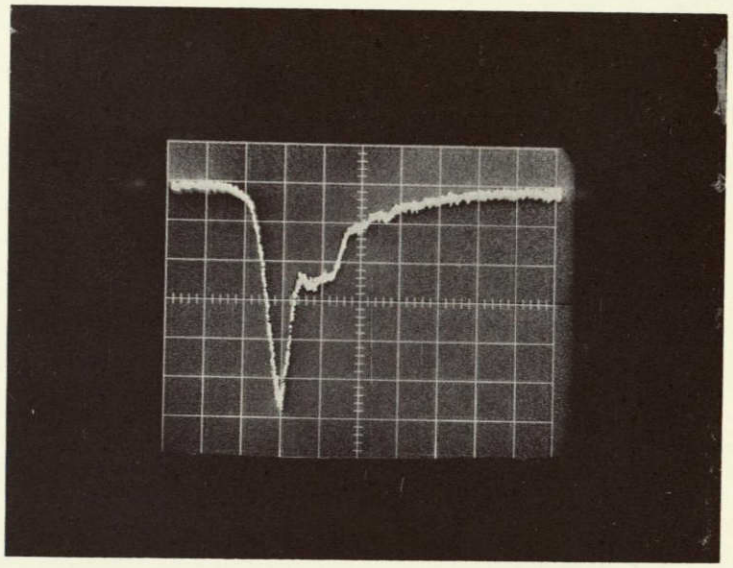

Figure 18. S/N 003 Pulse Response

Vertical Scale: 5 mv/div.
Horizontal Scale: 500 ps/div.

15 na Peak Cathode Current

REPRODUCIBILITY OF THE
ORIGINAL PAGE IS POOR

1.06 μ

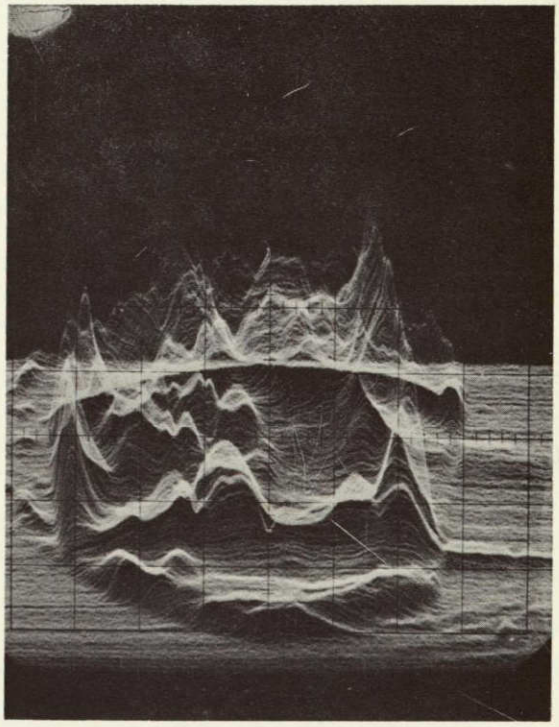

0.63 μ

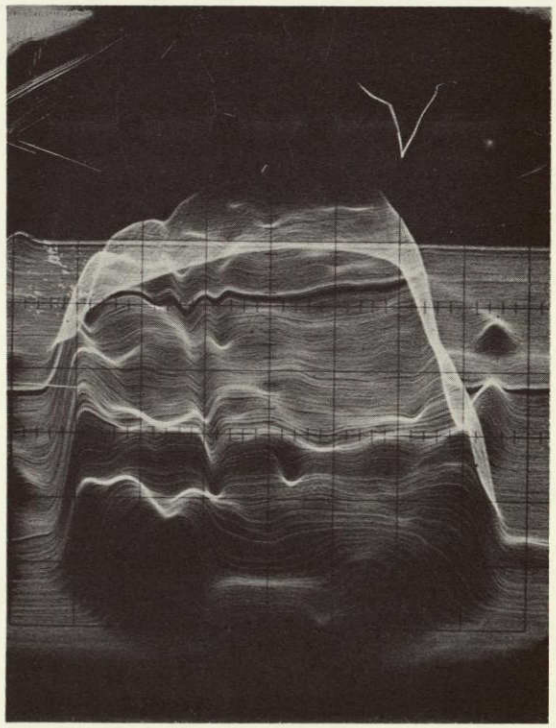

Figure 19. S/N 003 Cathode Scan at 1.06 μ and (0.63 μ) Laser Wavelengths

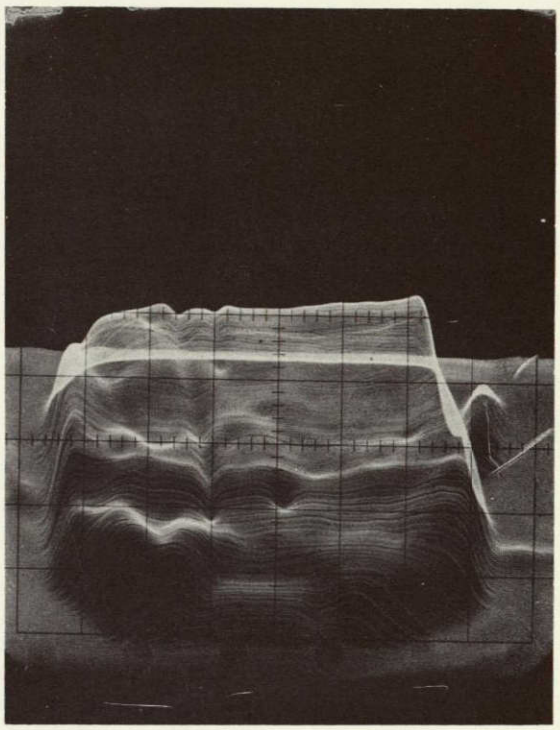

Figure 20. S/N 003 Gain Scan

S/N 006. This tube was started on 9/4/73 and received a 2% cathode. Cathode stability for this tube was very poor due to excessive Cs, even though the amount of Cs was reduced from that of S/N 003. It was surmized that the presence of the Cs generator was affecting stability. The Cs generator was therefore pinched off, but the tube went to air at this point and was scrapped.

S/N 007. Start date for this tube was 9/10/73. It received only a 1% QE cathode, but tube stability was significantly improved and this time the tube suffered from a shortage of Cs. Additions of Cs indicated stability over a period of one week at 0.7% QE, but a high voltage arc during testing and subsequent scrubbing reduced this yield to only 0.25%; however, stability looked good over a 2 week period at this level. In preparation for tube potting, this tube also went down to air upon Cs generator pinchoff. It was decided that the above failure was due to the fact that the copper was not cold welding during pinchoff due to a buildup of Cs_2O on the internal copper surface. Further pinchoffs of Cs generators were therefore curtailed until a solution could be developed.

S/N 008. This tube was started on 9/17/73. It received a preprocess that further reduced the Cs pressure level, since it appeared from S/N 007 that it is best to be Cs-lean. S/N 008 received a 4% cathode in October and clearly required additions of Cs to achieve stability. However, dumping the cathode response severely with Cs produced a significant improvement in stability at high QE. While having degraded a full 50% in infrared yield after 3 days following pinchoff, the tube was stable at 3% QE at 1.06 μ for three weeks following a Cs treatment and lost little response as a result of 50 μ operational scrubbing. To prevent the possibility of loosing this tube on Cs generator pinchoff, it was potted this time, leaving the generator in place physically sticking out beyond the tube housing. In this condition, the tube was tested at MDAC but unfortunately a high voltage arc that occurred during the testing setup drastically reduced the QE to only 0.1%. Figure 21 shows a 1.06 μ cathode scan with the uneven appearance of S/N 003. The cause of this is again explained by the serious cathode degradation.

REPRODUCIBILITY OF THE
ORIGINAL PAGE IS POOR

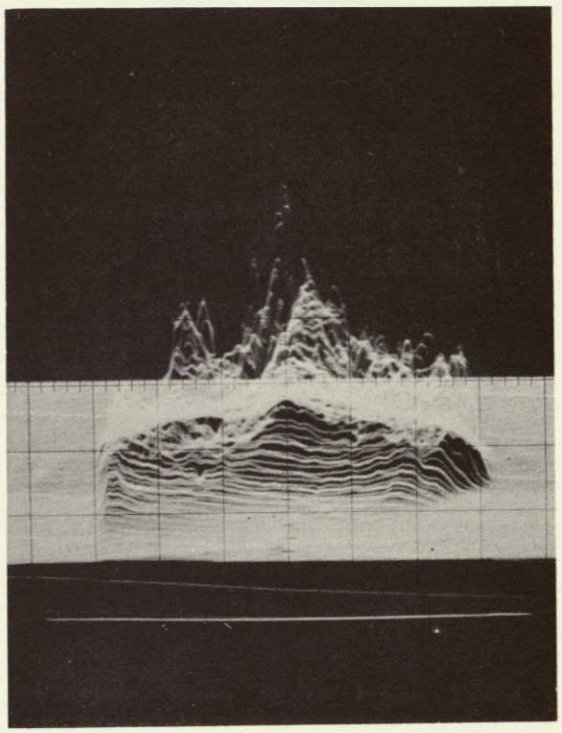

Figure 21. S/N 008 1.06 μ Cathode Scan

Figure 22 shows the output pulse which is again characterized by a secondary tail pulse. Gold plating of the anode structure to improve this had not yet been tried.

S/N 009. This tube, started 10/8/73, was processed identically to S/N 008 except that the CsCu feedthru was heated during tube processing in an effort to prevent a Cs_2O buildup there. In this case, 5.5% QE at 1.06 μ was achieved in the pinched-off device and, after one Cs dump, stability looked good at 4% QE and 3% QE after scrubbing. This tube was the last device in this phase on which a Cs generator pinchoff was attempted prior to potting (this tube was potted before S/N 008) and again the tube was lost due to a pinchoff leak even though the pinchoff area had been heated. At this point, further pinchoff of Cs generators was halted until a clear solution could be achieved.

S/N 010. S/N 010 was started on 10/16/73 and received a 5% at 1.06 μ cathode. After a Cs treatment, it showed good stability at 3% QE. QE fell to 2.8% after scrubbing, but after a second Cs treatment prior to potting the QE failed to recover past 0.6% — apparently due to too much Cs. In this condition, it was tested at MDAC. Figure 23 shows the pulse response, which was slightly better than 0.008, but much worse than expected since this tube had a gold-plated collector structure. A 1.06 μ cathode scan is shown in Figure 24. Peak QE is 0.6% at 1.06 μ and 0.5% average over 0.1" diameter. This response slowly degraded to 0.4% over the next six weeks and another Cs dump was performed. Four months later, the cathode had improved back to 0.5%.

S/N 011. This tube was started at Central Research on 11/1/73 to increase the tube start rate. It received a 4% cathode that degraded seriously and did not respond to a Cs treatment. The tube was subsequently scrapped.

S/N 012. S/N 012 was started on 10/29/73 and incorporated two changes. First, the collector structure position was changed about 0.30" towards the cathode in an effort to improve pulse response on the theory that signal current was missing the collector plate. Also, the preprocess was modified

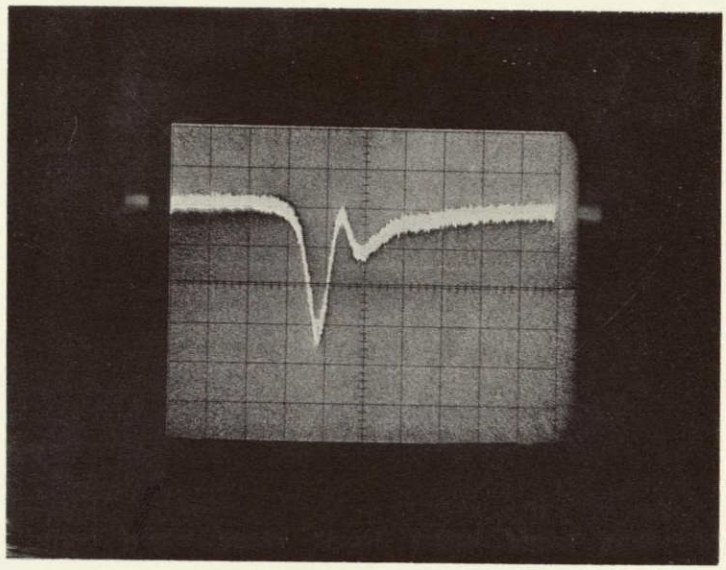

Figure 22. S/N 008 Pulse Response

Vertical Scale: 5 mv/div.
Horizontal Scale: 500 ps/div.

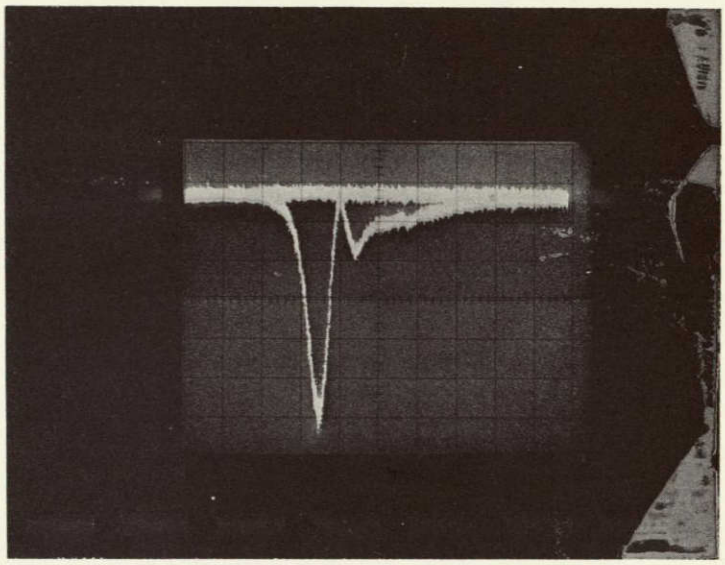

Figure 23. S/N 010 Pulse Response

Vertical Scale: 5 mv/div.
Horizontal Scale: 500 ps/div.

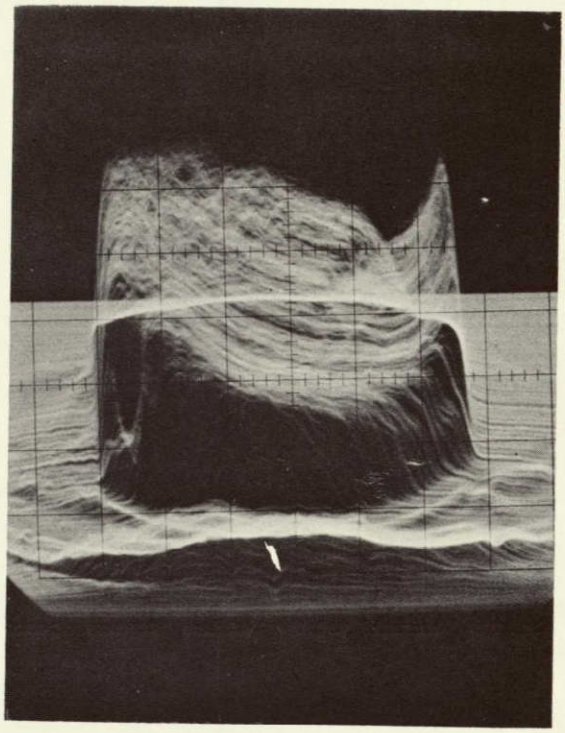

Figure 24. S/N 010 1.06 μ Cathode Scan

slightly to increase the Cs pressure to determine if the requirement for later Cs treatments would be reduced. The tube received a 5.5% QE cathode that required oxygen treatment this time. Stability was good at 2.5% after scrubbing and the tube was tested at MDAC with 2% QE at 1.06 μ. A cathode scan at 1.06 is shown in Figure 25. The poor uniformity is probably the result of cathode growth nonuniformity, although this could not be seen optically. Pulse response is shown in Figure 26; no improvement was indicated here, and a collector redesign was decided upon. The cathode sensitivity of this tube was not at all affected by testing at MDAC and remained stable at 1.6% QE for 1-1/2 months. At this point, degradation began. A Cs treatment then produced a stable yield at 0.8%. This tube was the first deliverable item for this phase.

S/N 013. This was the second tube to be processed at Central Research. It was started on 12/2/73 and received a 3% at 1.06 μ cathode. Cathode stability for this tube was much better than the last Central Research tube (S/N 011), but not as good as earlier tubes. Excessive Cs was the case for this device and it was clear at this point that the optimum preprocess for the Central Research vacuum system was considerably different than that for LSE Division's systems, possibly because of either a lower pumping speed or difference in bake-out oven design and use. Oxygen treatments stabilized cathode yield at 1%, while scrubbing reduced this to 0.8%. Further oxygen showed promising results, with a return to a stable 1%. However, the tube was lost this time on the oxygen pinch-off, again due to excessive Cs_2O on the copper surfaces.

S/N 014. S/N 014 was started on 11/5/73 and had the same preprocess as S/N 012. Apparently, this preprocess is very close to the correct one, since the initial 3% cathode was quite stable and slight oxygen treatment resulted in a constant 2-1/2% over a 3-week period. Scrubbing drastically reduced this yield to only 0.8%. These data indicated the need for further improvements in the UV scrubbing procedure that occurs during vacuum processing.

REPRODUCIBILITY OF THE
ORIGINAL PAGE IS POOR

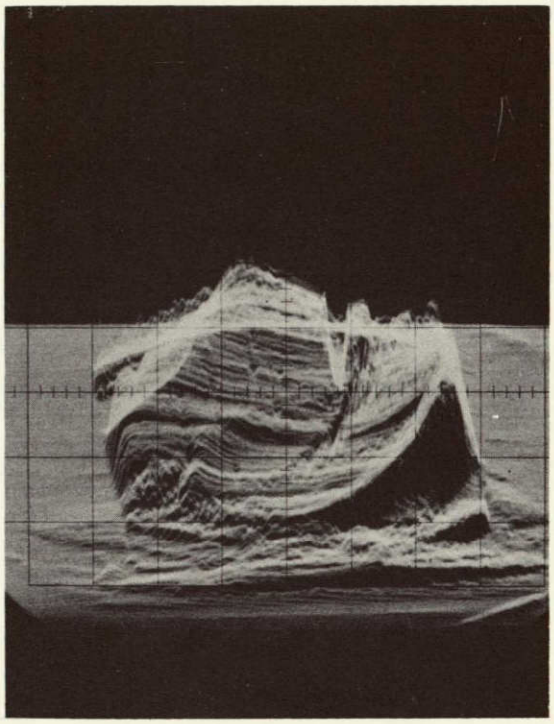

Figure 25. S/N 012 1.06 μ Cathode Scan

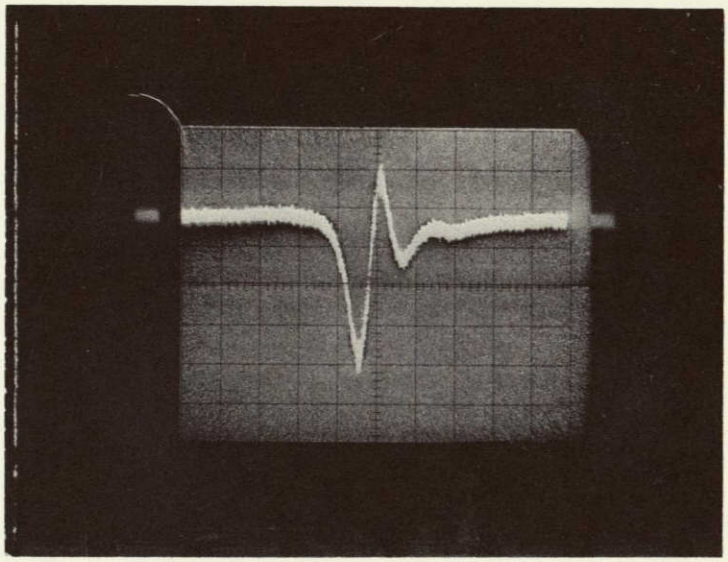

Figure 26. S/N 012 Pulse Response

Vertical Scale: 5 mv/div.
Horizontal Scale: 500 ps/div.

After the degradation resulting from scrubbing, the tube quickly degraded further without operation, apparently from a lack of Cs, since addition of Cs followed by a Cs dump resulted in a slow 9-week recovery to 1% QE. The sensitivity remained at that level for 3 months. S/N 014 became the second deliverable unit under this phase.

The eleven tube starts addressed above are summarized below in Table 1. This work effort successfully demonstrated that greater than 5% QE at 1.06 μ is achievable in an electrostatic PMT design that can easily handle 400 mb/s communication rates. Major problems are cathode shelf life, operating life and pulse response. Shelf life times of many months were indicated if the preprocess atmosphere was such that Cs treatments could later be applied. Long-term operating life data were not taken, but stable operation over a few hours was sometimes a problem with significant degradation occurring in some tubes, while some were stable. Pulse response was deteriorated in all cases by afterpulsing from secondary emission effects; a design modification is required before the problem could be eliminated.

B. PHASE II — TUBE PRODUCTION FOR SYSTEM AND LIFE TESTS

The work on this phase covered a 12-month period. The objective here was to deliver two all-electrostatic, high-speed detectors with an improved collector design for system testing at McDonnell-Douglas, followed by the delivery of two of the same type units after life testing. To accomplish this, the tube design of Phase I was modified to include a "honeycomb" collector design to eliminate afterpulsing that was noted earlier. This design was constructed and confirmed, and then further tubes were made for system and life testing. While no photocathode development was called for in this phase, significant further cathode studies were performed because of serious QE difficulties incurred during tube production.

TABLE 1

PHASE I TUBE SUMMARY CHART

Tube S/N	Start Date	Initial Gain	Scrub Current	Final Gain	Initial QE	QE After 50μA Scrub	Final QE	Comments
003	7/26/73	7×10^3	500 μA at Collector	6×10^3	3%	1.5%	0.04%	Poor preprocess atmosphere
005	8/23/73	-	-	-	-	-	-	Scrapped - tubulation fracture
006	9/4/73	5×10^3	600 μA at D5	3×10^3	2%	N.A.	-	Scrapped - down to air on Cs pinchoff
007	9/10/73	3.4×10^3	750 μA at D5	1×10^3	1%	0.25%	-	Scrapped - down to air on Cs pinchoff
008	9/17/73	3.5×10^3	200 μA at Collector	2×10^3	4%	2.8%	0.01%	Good stability - arced during testing at MDAC
009	10/8/73		200 μA at Collector		5.5%	3%	-	Scrapped - down to air on Cs pinchoff
010	10/16/73	1×10^4	200 μA at Collector	6×10^3	5%	2.5%	0.6%	Good initial stability - poor response to later cesiation
011	11/1/73	1×10^4	200 μA at Collector	-	4%	-	-	Processed at Central Research, poor preprocess, scrapped
012	10/29/73	8×10^3	200 μA at Collector	3×10^3	5.5%	2.5%	0.8%	Good stability
013	12/2/73		200 μA at Collector		3%	0.8%	-	Processed at Central Research, down to air on O_2 pinchoff
014	11/5/73	2×10^4	200 μA at Collector		3%	0.8%	1%	Best long-term stability

1. Device Development

The Phase I collector design is shown in Figure 27. The resultant collector response to a 300 ps laser pulse input appears in Figure 28. The positive pulse appearing immediately after the negative primary pulse is caused by secondary electrons generated on the collector plate leaving the collector structure and traveling to the ground mesh or beyond. To eliminate this problem, the flat collector plate was replaced with a honeycomb structure as shown in Figure 29. In this structure, the collector is made of a plurality of 0.005" holes about 0.050" deep. Electrons which enter these holes generate secondaries where they collide. Since the secondaries are generated in a hole, it is difficult for them to leave the structure, and by far the majority of secondaries simply hit the walls of the hole in which they are generated and are thereby captured. This new design successfully eliminated afterpulsing, as will be shown later.

Two other significant design changes occurred in Phase II. The first of these was the incorporation of an internal Cs generator within each tube instead of employing outside Cs generators (see Figure 14) which had to be pinched off before potting. The driving force that necessitated the change was the fact that a high percentage of Phase I tubes went down to air when the Cs generator was pinched off. This happened due to a buildup of Cs_2O on the 1/4" diameter copper walls of the tubulation between the generator and the tube, which prevented cold welding of the copper during pinchoff. Since it was not well understood how to prevent this situation without seriously affecting the delicate tube preprocess, it was decided in this phase to simply place the Cs channel within the tube enclosure. This immediately eliminated pinchoff problems, but introduced new difficulties. The presence of the Cs channel within the tube exposes it directly to oxygen treatments. It was discovered that use of the Cs channel after placement of the III-V cathode within the tube caused permanent cathode degradation. Although it was first thought that the channel was evaporating the Cs-chromate powder directly on the cathode, it was later proven that oxygen desorption from the channel was occurring. Pre-outgassing of this oxygen prior to crystal transfer was the ultimate solution.

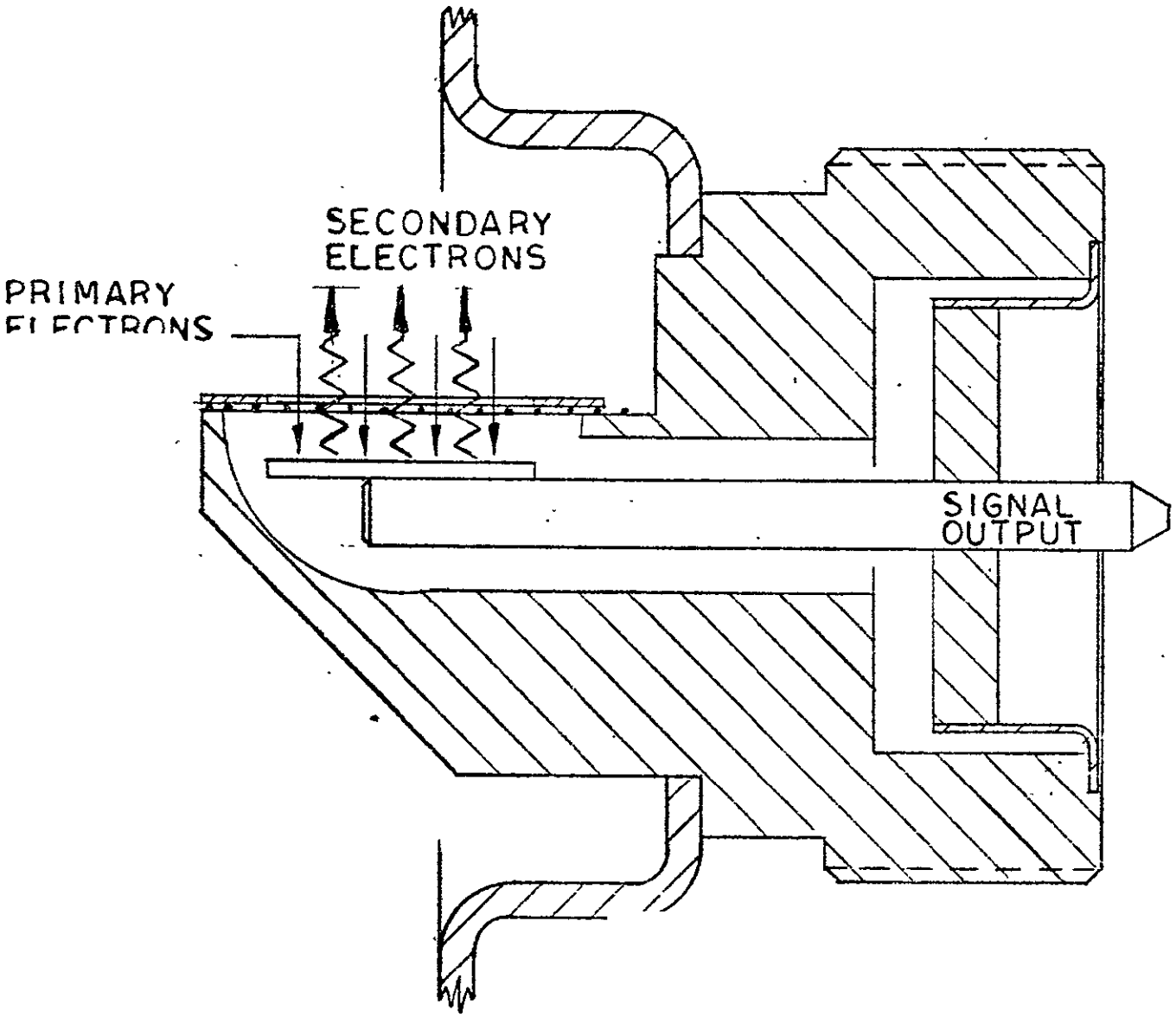

Figure 27. Phase I Collector Design

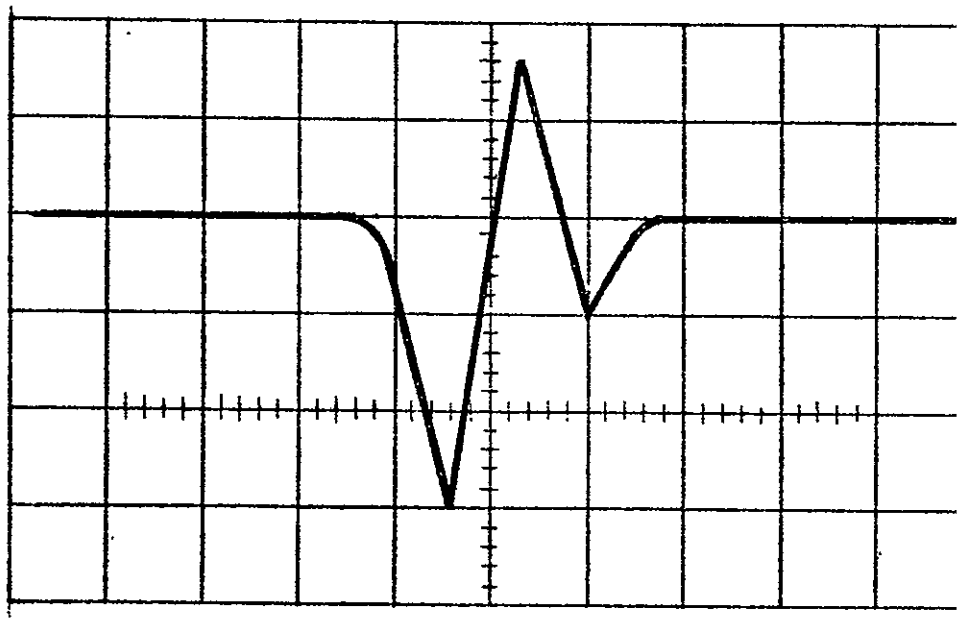

HORIZONTAL SCALE = 500 ps/DIV

VERTICAL SCALE = 5 Mv /DIV

Figure 28. Typical Phase I Collector Pulse

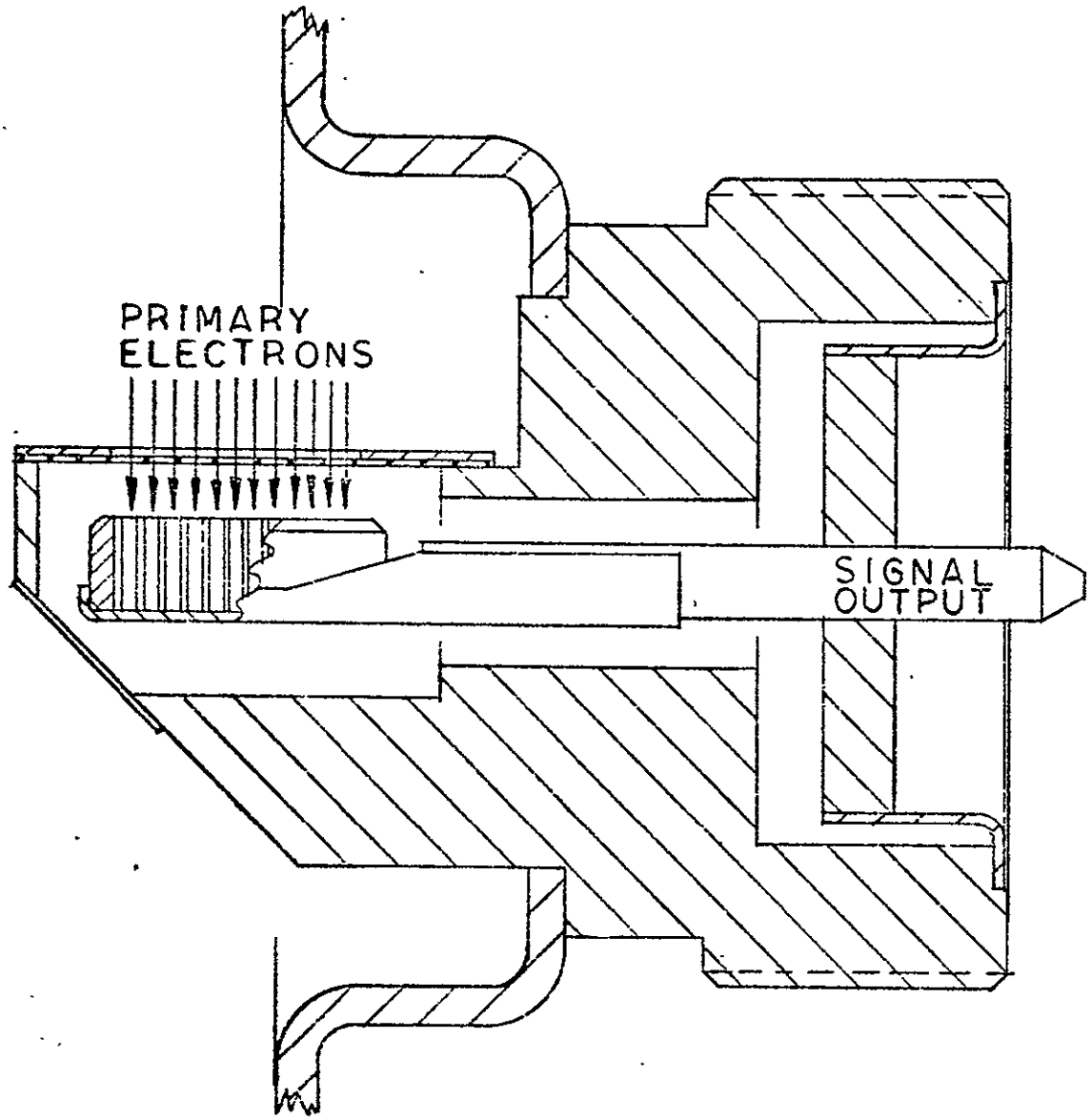

Figure 29. "Honeycomb" Collector Structure

The final significant design change which occurred during Phase II was a switch from five BeCu dynode stages to six dynode stages. The reason for this was to possibly improve tube performance in system testing, since 10^4 gain was desired by MDAC, while five-stage tubes produced only $\sim 2 \times 10^3$ gain. The change proceeded smoothly and had little effect on the pulse performance of the tube.

During this phase, severe cathode quality problems existed which greatly perturbed the flow of tube production. At the start of the work effort for Phase II, the LSE Division begain InGaAsP growth at its own facility in contrast to the prior technique of material growth at Central Research and subsequent transport of cleaned cathodes to LSE. The LSE growth system is shown in Figure 30. The first cathodes grown in this system achieved 3-1/2% QE at 1.06 μ, and yields greater than 5% were expected in a short time. However, subsequent yields were much poorer; and despite careful reoptimization of Zn doping levels and even a return to cathode growth at Central Research, over six months passed before 5% QE was again demonstrated. It was apparent that the QE difficulties experienced were caused by a multitude of problems, although vacuum system contamination appeared to be the most significant one since it resulted in a loss of accurate crystal quality feedback to our growth facilities. This resulted in a loss of optimum melt and doping composition so that poor results became progressively worse. Cathode yields improved again as a result of vacuum system cleaning along with a re-optimization of growth and handling procedures. The evaluation efforts of Central Research were crucial to this solution process, since their evaluation of LSE crystals allowed for reoptimization of the LSE material independent of LSE vacuum systems.

2. Individual Device Performance

Eight tube starts proceeded during Phase II. These starts yielded tubes for system testing at MDAC as well as life test samples. Each tube is described below.

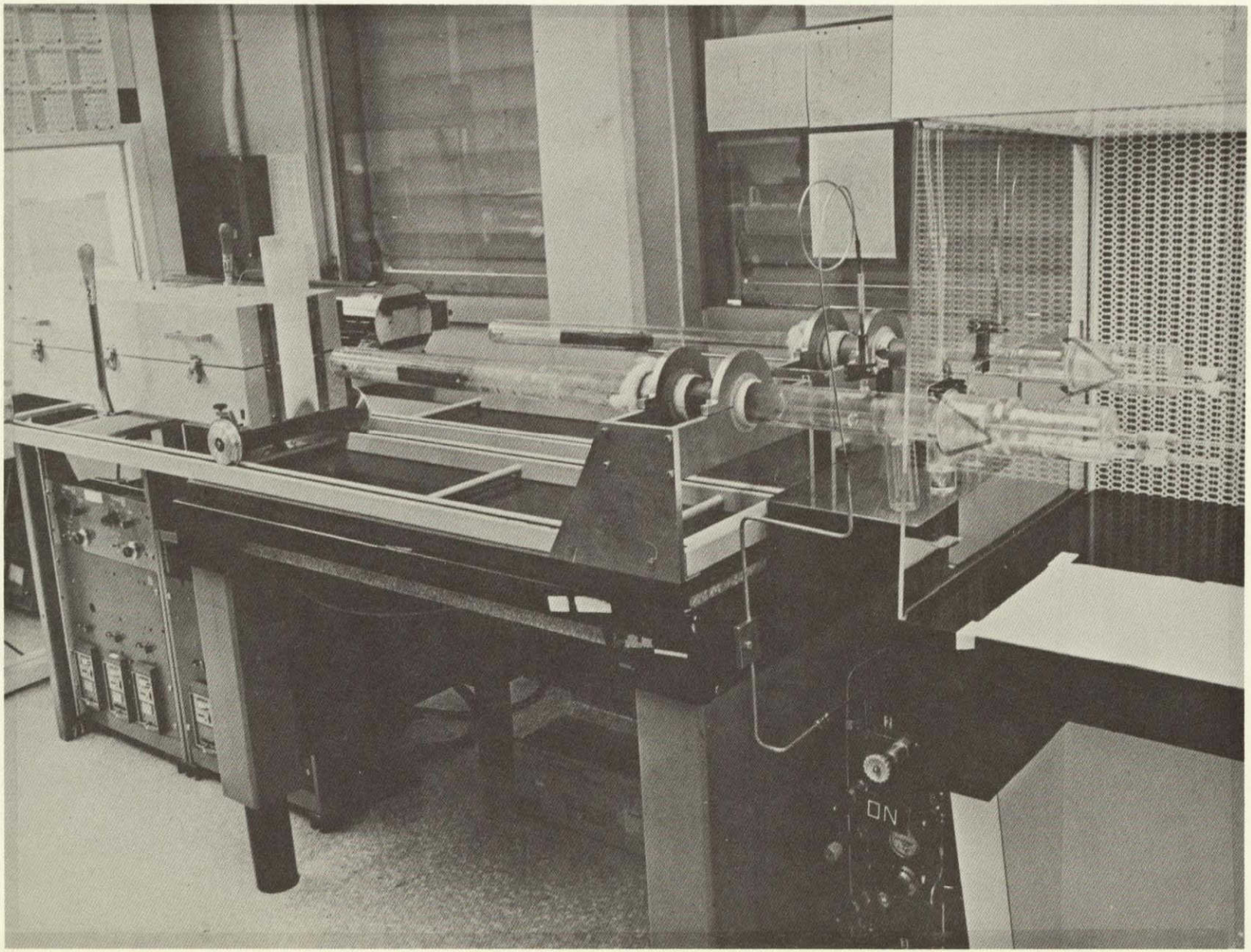

Figure 30. LSE III-V LPE Growth System

REPRODUCIBILITY OF THE
ORIGINAL PAGE IS POOR

S/N 027. This tube had five beryllium-copper dynodes and a "honeycomb" collector. It was started on 5/31/74 and received bakeout and preprocess procedures identical to those developed on Phase I. However, an internal Cs generator was used in this and subsequent tubes and, therefore, further preprocessing refinements would probably be required. A 2.8% cathode was placed in this tube and good stability was achieved at 1.5%, but scrubbing reduced this yield to only 0.02% and there was no recovery. It was felt that this degradation was the result of insufficient scrubbing during tube processing, and increased scrubbing currents were planned. Pulse response for this tube is shown in Figure 31. This MDAC data confirmed that the honeycomb collector was the answer to past problems with pulse performance. The speed of this tube was sufficient for 1 GB communication.

S/N 028. This tube was started on 7/2/74. It was the first tube to have six stages for high (10^4) gain and improved scrubbing flexibility. Initial gain was only 7×10^3 for this device so that increased scrubbing current (500 μA) could not be used without sacrificing final gains. 5.3% QE at 1.06 μ was achieved in this tube. However, preprocessing difficulties arose with this tube, as witnessed by the presence of excessive Cs and the subsequent need for oxygen treatments to stabilize the tube. S/N 028 was the first deliverable item for system testing of this phase and was shipped to MDAC with 1.5% QE at 1.06 μ and 4×10^3 gain. It subsequently arced, and QE degraded to 0.1% as a result.

S/N 028 caused significant dynode string optimization work to be performed. It was initially delivered to MDAC with an internal divider chain employing 2 megohms/stage with a 600 V Zener-controlled voltage on the last dynode. This circuit was established to provide a minimum amount of power dissipation in the divider chain to minimize tube heating effects, while still allowing for continuous tube collector currents of 50 μA. At MDAC, this circuit allowed only 15 to 20 μA of collector current. To alleviate this current-limiting condition, S/N 028 (along with S/N 029) was returned to Varian and the 2 megohm resistors were

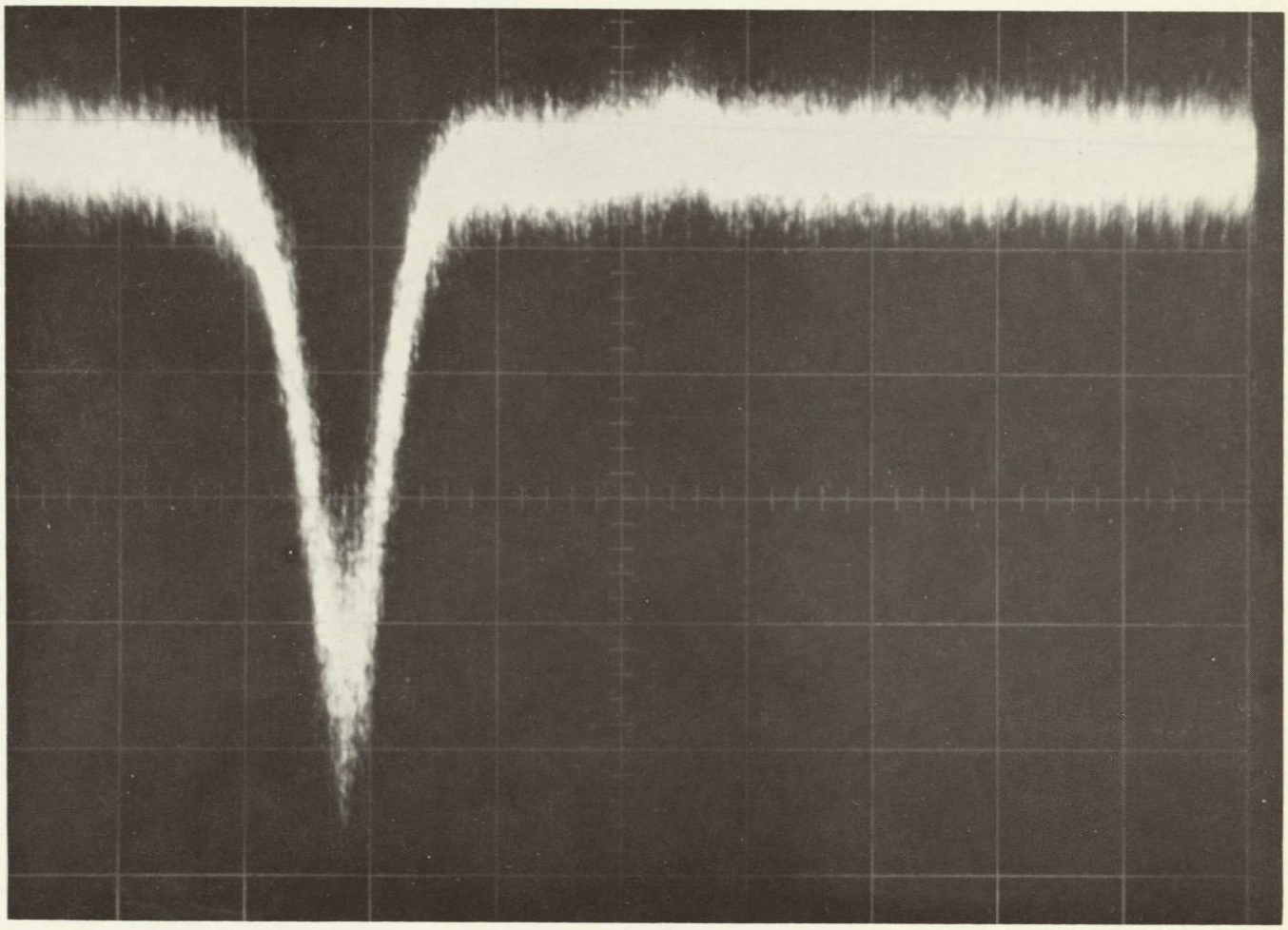

Figure 31. S/N 027 Output Pulse Response

Vertical Scale: 5 mv/div.
Horizontal Scale: 500 ps/div.

REPRODUCIBILITY OF THE
ORIGINAL PAGE IS POOR

replaced with 1 megohm resistors. Saturation current levels were still unacceptable due to current limiting occurring in the next-to-last dynode. This condition was corrected by applying Zener bias on this dynode as well. So, the final wiring configuration which provided the proper operating current levels became an integral divider chain employing 1 megohm per stage with 600 V Zener bias voltages on the last and next-to-last dynodes. Under this condition, total bleeder string current was 600 μA and total power dissipation was $\sim$ 2.5 W.

S/N 029. This tube was started on 7/19/74 and was preprocessed the same as S/N 028 (sufficient S/N 028 stability data were not yet available). Initial gain for this tube was 6×10^4, high enough for a 500 μA collector current scrub. This was performed, and gain after scrubbing fell to 1.5×10^4, which was considered at the time to be an ideal gain for system testing. A 5% at 1.06 μ cathode was placed in this tube, but the preprocess atmosphere exhibited excessive Cs as well and cathode stability was poor.

S/N 029 became the second deliverable tube in this phase and was subsequently shipped to MDAC. The same wiring difficulties that were experienced with S/N 028 occurred on this tube and the same solution was implemented.

S/N 030. S/N 030 was started on 8/12/74 and was preprocessed with less Cs to improve cathode stability over that of S/N 028 and 029. This tube was the first to be scrubbed at 500 μA of collector current, but with no limiting cathode aperture (0.5" compared to 0.1" in the past). The theory here was that the 0.100" scrub might miss some dynode areas and subsequent use of the tube under different conditions would result in electron bombardment of unscrubbed surfaces and, there, reduced operating life. An overnight scrub under this new condition reduced gain from 7×10^3 to only 1×10^3. Only a 2% at 1.06 μ cathode was injected into the tube. Six cathodes were tried but initial yields of the first five were all very poor. The best one was the sixth at 2%, so the cathode was used at this point to preclude further, possibly futile, efforts. Room temperature stability

of this tube was better than tubes of the recent past and indicated that S/N 030 would be a good life test candidate. In late September, stable shelf performance at 1% QE was achieved. In late October S/N 030 was wired in the final configuration of S/N 028 and 029. At rated output current (50 μA), the QE degraded from 1% QE at 1.06 μ to only 0.1% in just 30 minutes. The reason for this degradation was not the output current level, but the divider chain potted within the tube housing. While the use of a 1 M ohm resistor and Zener diode bias on the last two dynodes had previously eliminated collector current saturation problems, after 1/2 hour of operation the power dissipated by this divider caused the tube temperature to increase to 70°C. Such an increase in temperature has rapidly degraded InGaAsP cathodes in past experiments, and clearly did so here. It was then decided to provide future tubes with flying leads to bias the dynodes from an external divider (which is commonly done at McDonnell-Douglas with crossed field PMT's). This new configuration is also important from the standpoint of noise performance, since it was discovered that the application of Zener diodes for biasing such tubes introduces system noise due to the high noise level of the high-voltage Zener diodes used in this application.

S/N 031. This tube, which was originally started on 8/15/74, was baked a total of five times as a result of two vacuum system failures and extreme difficulties in achieving acceptable QEs. The first cathodes were tried after the third bake in September, but it took 21 attempts and two more bakes to achieve 2% QE at 1.06 μ. This occurred in mid-November. Concurrently, S/N 031 became an experimental vehicle for studying yet another problem, that of internal Cs contamination of good cathodes. This tube and the following unit, S/N 032, both experienced severe cathode degradation after crystal transfer when the internal Cs generator was activated. The need for Cs additions is established by the preprocess sequence, since long room-temperature cathode life can be achieved in this way. However, when the proper preprocess sequence was finally achieved, additions of Cs for cathode rejuvenation immediately and permanently degraded cathodes even before Cs was liberated. It was first thought that something was evaporating from the Cs channel directly onto the cathode, since it was in full view of the Cs channel. So, on the last

bake of S/N 031, the channel was routed behind the cathode holder and therefore not in view of the cathode. The contamination condition continued with no change, however, thus proving that the contamination is a gaseous one that occurs when the Cs channel is heated. It was further shown on S/N 031 that preflashing (or pre-firing) the Cs channel prior to cathode transfer eliminates this problem.

S/N 031 was finally pinched off in late November with a 2% cathode, which was the best that could be achieved. Although the Cs channel was working properly for this tube, within only 3 days the cathode response fell a factor of 10 and did not respond to any treatment. This condition must have been the result of the presence of a contaminant gas and not a leak in the tube, since the cathode slowly recovered to 0.3% by March 1975.

S/N 032. This tube was started on 10/10/74 and, after six cathode attempts, only 2% QE at 1.06 μ was achieved. The continued problems with cathode yields prompted a cessation of tube starts (two remained) until cathode yields of 5% at 1.06 μ could again be achieved. S/N 032 responded poorly to Cs treatment due to the aforementioned Cs generator outgassing problem that was diagnosed by experiments with S/N 031. In the case of S/N 032, the Cs treatment attempt 3 days following pinchoff drastically reduced cathode yield to 0.1%, and no recovery followed. The occurrence of this type of cathode degradation led to a new vacuum processing procedure. It was decided that when a high-yield cathode is transferred into each tube, it would not be locked into place, but instead would be seated lightly into the tube crystal holder. After its stability was ascertained the cathode would be locked into place and subsequently the tube would be pinched off the vacuum system. Although this procedure was difficult and time-consuming, it would significantly increase the likelihood of achieving a stable device after pinch-off.

To improve cathode yields, a dual approach was undertaken. First, any InGaAsP material grown at LSE received evaluation at Central Research, and would continue to do so until the proper optimization could be achieved. This

procedure eliminated possible LSE vacuum system problems from interfering with the optimization process. By the end of December, better than 3%QE was achieved and data indicated that better than 5% would be achieved soon thereafter.

The second solution approach was based on the assumption that the two LSE III-V vacuum processing systems might have been contaminated to the point where they had been limiting the achieved QE from good cathode material. Therefore, both vacuum systems were disassembled, cleaned and reassembled.

In late February, 5% QE material was finally demonstrated at LSE and the remaining two starts were begun. It was apparent that the QE difficulties experienced over these past few months were caused by a multitude of problems, although vacuum system contamination appeared to be the most significant one since it resulted in a loss of accurate crystal quality feedback to our crystal growth facility. This resulted in a loss of optimum melt and doping composition, as described earlier. By February, both available vacuum systems were in excellent condition and all crystal growth and handling procedures had been re-optimized back to a controlled operation so that tube starts could be resumed.

S/N 035. S/N 035 was started on 5/2/75. (S/N 035 and 036 starts were delayed because it was decided to wait for an indication from MDAC that they were ready for final system tests.) Go-ahead was received in early April (S/N 036 was started first). S/N 035 was scrubbed at 1 mA of collector current to reduce tube gain to about 3×10^3, since it was felt that this gain was more appropriate than 10^4 gain for optical communication system performance (this decision was the result of the preliminary system testing performed earlier at MDAC). In mid-May, a 5% QE at 1.06 μ cathode was transferred into this tube and after pinchoff and scrubbing, 3.5% was achieved. The tube was subsequently provided for system tests as the final deliverable item under this program. It was delivered in a thermoelectric cooler which operated the tube at -20° C for reduced dark current and better cathode stability (cathode shelf life is improved X 1000 by

cooling to -20°C). In addition, individual dynode leads were provided to prevent tube heating from divider power dissipation and also to remove Zener diodes from the biasing circuit due to their noisy operating characteristics which impair system BER performance. System testing of S/N 035, which had the highest delivered QE, indicated that the tube performance is limited by an ion feedback noise condition. After the tube was returned to Varian following testing, QE had degraded below 2% at 1.06 μ (this tube had excess Cs in the atmosphere due to Cs generator preflashing which altered the preprocess from its optimum condition). The cathode continued to degrade to 0.65% in September 1975 since rejuvenation could not be pursued because the oxygen source had been pinched off prior to tube potting in May. However, it was felt that a -20°C life test could be performed at this point to assess operating stability at 50 μA of output current. Figure 32 shows the result of a 38-day (~ 900 hrs) life test. Here, operation reduced sensitivity to only 0.035%. These data indicate that even 1 mA scrubbing appears to be insufficient for stable operation at high 1.06 μ sensitivity, or possibly that the presence of ion feedback to the photocathode disrupts the Cs_2O coating, thereby reducing cathode QE.

S/N 036. This tube was started on 4/8/74 and had an excellent initial gain of 2×10^5 (the highest of this series). It was scrubbed at 500 μA of collector current overnight and gain stabilized at 2×10^4 (indications that lower tube gain might improve system performance had not yet been received from MDAC). A 3.5% QE cathode was placed in this tube. S/N 036 responded well with Cs after pinchoff and appeared to be an excellent candidate for system and life testing. However, due to a wiring error during setup for scrubbing, the focus slot for the sixth dynode arced to the sixth dynode and degraded the cathode to << 0.1% at 1.06 μ.

The eight tube starts of this phase are summarized in Table 2. The most significant result of this effort was the demonstration of competitive system BER performance with a high speed 1.06 μ PMT, even in the presence of a signal induced noise mechanism. The major problems which were identified

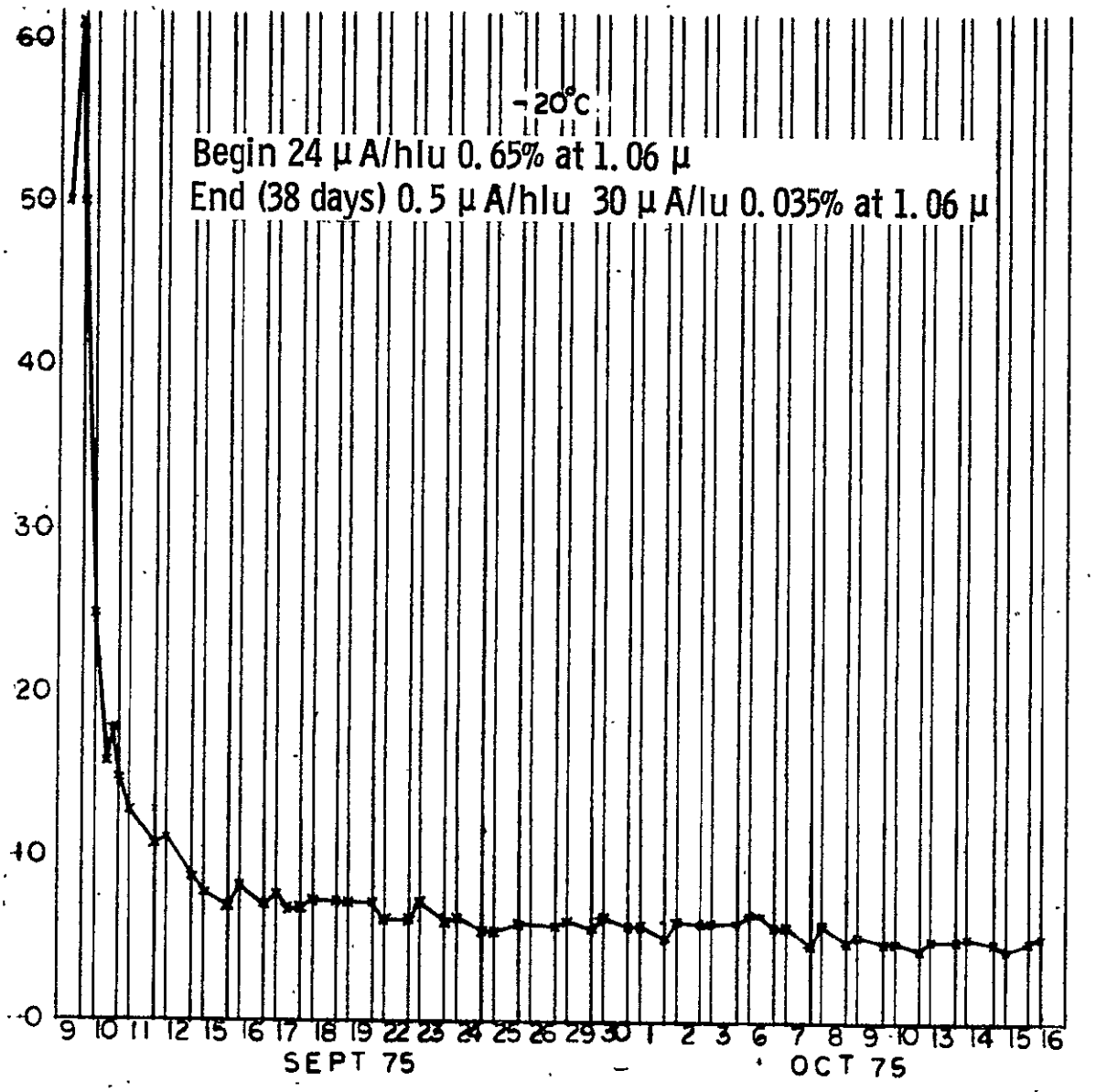

Figure 32. S/N 035 50 μA Output Current Life Test

TABLE 2

PHASE II TUBE SUMMARY CHART

Tube S/N	Start Date	Initial Gain	Scrub Current	Final Gain	Initial QE	QE After 50 μA Scrub	Final QE	Comments
027	5/31/74	8×10^3	250 μA at Collector	3×10^3	2.8%	0.07%	0.01%	Poor preprocess
028	7/2/74	7×10^3	250 μA at Collector	4×10^3	5.3%	1.5%	0.1%	Poor preprocess; arced during MDAC testing
029	7/19/74	6×10^4	500 μA at Collector	7×10^3	5%		0.4%	
030	8/12/74	7×10^3	500 μA at Collector (no aperture)	1×10^3	2%	1%	0.1%	Good preprocess. Got to 70°C during life test
031	8/15/74	1×10^5	500 μA at Collector	9×10^3	2%	0.1%	0.3%	Possible vacuum contamination - preflashed Cs
032	10/10/74	1.5×10^4	500 μA at Collector	6×10^3	2%	0.1%	0.1%	Cathode contaminated by use of Cs generator
035	5/2/75	6.5×10^4	1 mA at Collector	3×10^3	5%	3.5%	3.5%*	Used for system test at -20°C
036	4/8/75	2×10^5	500 μA at Collector	2×10^4	3.5%	Not Performed	<0.1%	Arced during setup for scrubbing

*QE at delivery to MDAC in 5/75
QE was 0.65% at Varian in 9/75 and
0.035% after 38-day life test

through this effort were operating stability as well as signal-induced noise (ion feedback). Further engineering efforts are indicated in these two areas. Also, problems in achieving high cathode yields and in the use of integral Cs channels were addressed, with significant progress being achieved in both areas; but follow-up efforts are still required.

APPENDIX A

PUBLICATIONS

PUBLICATIONS

The following are publications by Varian personnel in the area of III-V compound technology, of relevance to the proposed program.

1. J. J. Uebbing and R. L. Bell, "Cesium-GaAs Schottky Barrier Height," Appl. Phys. Letters 11, 357 (1967).

2. R. L. Bell and J. J. Uebbing, "Photoemission from InP-Cs-O," Appl. Phys. Letters 12, 76 (1968).

3. J. J. Uebbing and R. L. Bell, "Improved Photoemitters Using GaAs and InGaAs," Proc. IEEE 56, 1624 (1968).

4. L. W. James (with J. L. Moll and W. E. Spicer), "The GaAs Photocathode," Proc. 1968 Symp. on GaAs (Conf. Series #7, IPPS, London, 1969), pp. 230-237.

5. L. W. James (with R. C. Eden, J. L. Moll, and W. E. Spicer), "Location of the L_1 and X_3 Minima in GaAs as Determined by Photoemission Studies," Phys. Rev. 174, 909 (1968).

6. L. W. James (with J. L. Moll), "Transport Properties of GaAs Determined from Photoemission Measurements," Phys. Rev. 183, 740 (1969).

7. R. L. Bell, "Thermionic Emission of the GaAs Photocathode," Solid State Electronics 12, 475 (1969).

8. J. J. Uebbing, L. W. James, and G. A. Antypas, "Improved Photocathodes for 1.06 Micron Detection Using $GaAs_{1-x}Sb_x$-Cs_2O," Proc. of DoD Laser Conference, January 1970.

9. J. J. Uebbing, "Use of Auger Electron Spectroscopy in Determining the Effect of Carbon and Other Surface Contaminants on GaAs-Cs-O Photocathodes," J. Appl. Phys. 41, 802 (1970).

10. J. J. Uebbing (with N. J. Taylor), "Auger Electron Spectroscopy of Clean Gallium Arsenide," J. Appl. Phys. 41, 804 (1970).

11. J. J. Uebbing, "Auger Electron Spectroscopy of Contaminated Gallium-Arsenide Surfaces," J. Vac. Sci. Technol. 7, 81 (1970).

12. T. O. Yep (with R. J. Archer), "Dependence of Schottky Barrier Height on Donor Concentration," J. Appl. Phys. 41, 303 (1970).

13. G. A. Antypas and L. W. James, "Liquid Epitaxial Growth of GaAsSb and Its Use as a High-Efficiency, Long-Wavelength Threshold Photoemitter," J. Appl. Phys. 41, 2165 (1970).

14. R. L. Bell, "Thermionic Emission from 3-5 Infrared Photocathodes," Solid State Electronics 13, 397 (1970).

15. G. A. Antypas, "The Ga-GaP-GaAs Ternary Phase Diagram," J. Electrochem. Soc. 117, 700 (1970).

16. L. W. James and J. J. Uebbing, "Long Wavelength Threshold of Cs_2O-Coated Photoemitters," Appl. Phys. Letters 16, 370 (1970).

17. L. W. James (with J. P. Van Dyke, F. Herman, and D. M. Chang), "Band Structure and High Field Transport Properties of InP," Phys. Rev. B 1, 3998 (1970).

18. G. A. Antypas, L. W. James, and J. J. Uebbing, "Operation of III-V Semiconductor Photocathodes in the Semitransparent Mode," J. Appl. Phys. 41, 2888 (1970).

19. J. J. Uebbing and L. W. James, "Behavior of Cs_2O as a Low Work Function Coating," J. Appl. Phys. 41, 4505 (1970).

20. G. A. Antypas, "Liquid-Phase Epitaxy of $In_xGa_{1-x}As$," Electrochem. Soc. 117, 1393 (1970).

21. R. L. Bell (with W. E. Spicer), "3-5 Compound Photocathodes: A New Family of Photoemitters with Greatly Improved Performance," Proc. IEEE 58, 1788 (1970).

22. L. W. James, G. A. Antypas, J. J. Uebbing, T. O. Yep, and R. L. Bell, "Optimization of the $InAs_zP_{1-x}$-Cs_2O Photocathode," J. Appl. Phys. 42, 580 (1971).

23. L. W. James, G. A. Antypas, J. J. Uebbing, J. Edgecumbe, and R. L. Bell, "III-V Ternary Photocathodes," Gallium Arsenide and Related Compounds (Conf. Series #9, IPPS, London, 1971), p. 195.

24. G. A. Antypas and T. O. Yep, "Growth and Characterization of Liquid-Phase Epitaxial $InAs_{1-x}P_x$," J. Appl. Phys. 42, 3201 (1971).

25. R. L. Bell, "R&D on 3-5 Photocathodes," Invited Paper, PSEE Conference, U. of Minnesota, August 18-19, 1971.

26. L. W. James, G. A. Antypas, R. L. Moon, and R. L. Bell, "The Effects of Stress on Cs_2O-Activated III-V Photocathodes," PSEE Conference, U. of Minnesota, August 18-19, 1971.

27. L. W. James, G. A. Antypas, J. Edgecumbe, R. L. Moon, and R. L. Bell, "Dependence on Crystalline Face of the Band Bending in Cs_2O-Activated GaAs," J. Appl. Phys. 42, 4976 (1971).

28. R. L. Bell, L. W. James, G. A. Antypas, J. Edgecumbe, and R. L. Moon, "Interfacial Barrier Effects in III-V Photoemitters," Appl. Phys. Letters 19, 513 (1971).

29. R. L. Bell (with W. E. Spicer), "The III-V Photocathode: A Major Detector Development," Pub. Astron. Soc. Pacific 84, 110 (1972).

30. G. A. Antypas, "Liquidus and Solidus Data at 500°C for the In-Ga-Sb System," J. Crystal Growth 16, 181 (1972).

31. G. A. Antypas, R. L. Moon, L. W. James, J. Edgecumbe, and R. L. Bel "III-V Quaternary Alloys" in Gallium Arsenide and Related Compounds 1972 (IPPS, London, 1973), p. 48.

32. L. W. James, G. A. Antypas, R. L. Moon, J. Edgecumbe, and R. L. Bell, "Photoemission from Cesium-Oxide-Activated InGaAsP," Appl. Phys. Letters 22, 270 (1973).

33. R. D. Fairman (with R. Solomon), "Submicron Epitaxial Films for GaAs Field Effect Transistors," J. Electrochem. Soc. 120, 541 (1973).

34. R. L. Moon and L. W. James, "Auger Spectra of HCl Vapor-Etched n^+ GaAs {100} Substrates," J. Electrochem. Soc. 120, 581 (1973).

35. L. W. James, "Parameters of Electron Transfer in InP," J. Appl. Phys. 44, 2746 (1973).

36. R. L. Bell, Negative Electron Affinity Devices (Clarendon Press, Oxford, 1973).

37. R. L. Moon and G. A. Antypas, "Surface Irregularities due to Spiral Growth in LPE Layers of AlGaAs and InGaAsP," J. Crystal Growth 19, 109 (1973).

38. G. A. Antypas and R. L. Moon, "Growth and Characterization of InP-InGaAsP Lattice-Matched Heterojunctions," J. Electrochem. Soc. 120, 1575 (1973).

39. R. L. Moon (with J. Kinoshita), "Comparison of Theory and Experiment for LPE Layer Thickness of GaAs and GaAs Alloys," J. Crystal Growth 21, 149 (1974).

40. L. W. James, "Calculation of the Minority-Carrier Confinement Properties of III-V Semiconductor Heterojunctions (Applied to Transmission-Mode Photocathodes)," J. Appl. Phys. 45, 1326 (1974).

41. R. L. Bell, "GaAs Solar Cells for Terrestrial Power Generation," -- NSF (RANN) Solar Energy Conference, Tucson, Arizona, May 1974.

42. L. W. James and R. L. Moon, "GaAs Concentrator Solar Cell," submitted to Appl. Phys. Letters, November 1974.

43. L. W. James, "Materials Development for Large-Scale Economical Applications of Solar Cells--III-V Materials," Northern California Section of AIME, U. California, Berkeley, November 1974.

44. R. L. Moon, "The Influence of Growth Solution Thickness on the LPE Layer Thickness and Constitutional Supercooling Requirement for Diffusion-Limited Growth," J. Crystal Growth 27, 62 (1974).

45. R. L. Bell, L. W. James, and R. L. Moon, "Transferred Electron Photoemission from InP," Appl. Phys. Lett. 25, 645 (1974).

46. J. S. Escher, R. D. Fairman, G. A. Antypas, R. Sankaran, L. W. James, and R. L. Bell, "Field-Assisted Photoemission from an InP/InGaAsP/InP Cathode," Proc. Conference of the Physics of Compound Semiconductor Interfaces, to be published.

47. G. A. Antypas and J. Edgecumbe, "A Glass-Sealed GaAs-AlGaAs Transmission Photocathode," Appl. Phys. Lett. 26, 371 (1975).

48. L. W. James and R. L. Moon, "GaAs Concentrator Solar Cells," Proc. 11th IEEE Photovoltaic Specialists Conference, to be published.

49. R. L. Bell, "Selection Rules for Negative Affinity Emission," J. Phys. D: Appl. Phys. 8, L118 (1975).

50. R. L. Bell, "Noise Figure of the MCP Image Intensifier Tube," IEEE Trans. Electron Devices ED-22, 821 (1975).

APPENDIX B

VARIAN ELECTRON OPTICS COMPUTER PROGRAM

VARIAN ELECTRON OPTICS COMPUTER PROGRAM

The electron tube computer program that is utilized has successfully aided in the design of a wide variety of devices. It was designed to handle complex problems in electron optics and has provision for modeling systems with arbitrary spatial and energy distributions as initial conditions.

The program is of the analysis type; that is, given the electrode shapes, electrode potentials, and the emitting surface together with the appropriate initial conditions, the resultant beam (consisting of a number of representative trajectories) is traced through the electrode system. The program can handle electrodes having arbitrary potentials and arbitrary shapes in cylindrical geometry.

The general design of the program is shown in the flow chart in Figure B-1. The first user input to the program consists of a mesh size and a set of closed boundaries defined by data points at which potentials are specified.

The program overlays the region of concern with a rectangular mesh. The quantities of interest are assumed to vary in a relatively simple fashion between mesh points (stepwise or linear). A second user input consists of a number of representative trajectory origins chosen on the emitting surface, simulating electron emission. From each origin, a group of trajectories is specified that have a set of directed velocities chosen to best approximate an actual continuous distribution.

Next, Laplace's equation is solved for the potentials of each mesh point. A system of finite difference equations is constructed for the interior points of the mesh, and these are solved using successive over-relaxation techniques. Using this process, a highly accurate potential matrix is obtained from which the equipotentials can be computed.

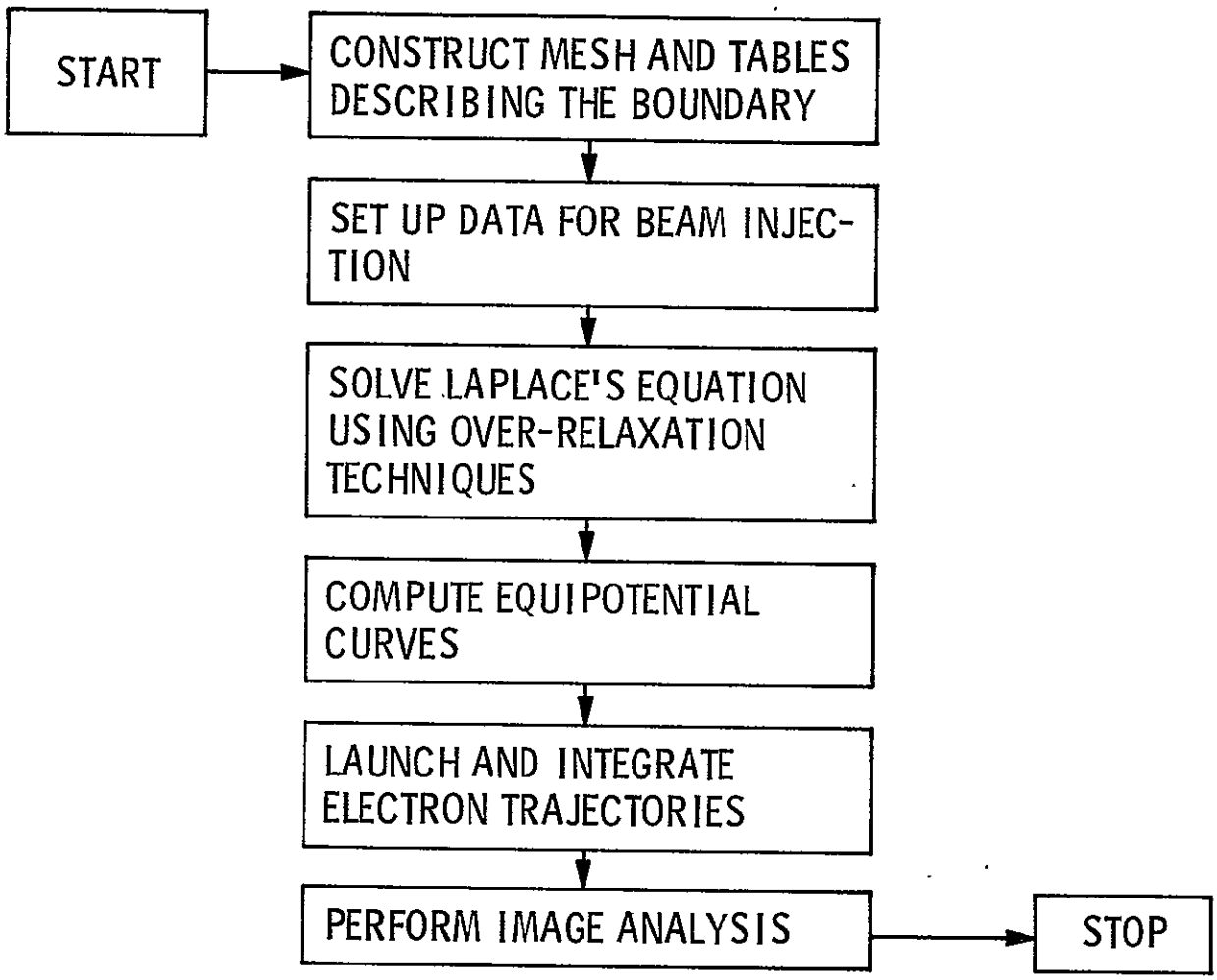

Figure B-1. Computor Program Flow Chart

The trajectories are then launched and traced through the electrode system using the differential equations that describe electron (or ion) flow in electric fields. The trajectory integration uses sophisticated numerical procedures, which provide a three-dimensional description of the beam behavior as a function of time. The approach is quite general; paraxial ray approximations are not assumed. The output of the program consists of a Calcomp plot of the prescribed boundary, the electron trajectories, and a set of equipotential lines.